ELSEVIER

Chemical Geology 241 (2007) 207–233

CHEMICAL GEOLOGY
INCLUDING
ISOTOPE GEOSCIENCE

www.elsevier.com/locate/chemgeo

The application of olivine geothermometry to infer crystallization temperatures of parental liquids: Implications for the temperature of MORB magmas

Trevor J. Falloon [a,*], Leonid V. Danyushevsky [b], Alexei Ariskin [c], David H. Green [d], Clifford E. Ford [e]

[a] *School of Earth Sciences and Centre for Marine Science, University of Tasmania, Private Bag 79, Hobart, Tasmania 7001, Australia*
[b] *School of Earth Sciences and Centre for Ore Deposit Research, University of Tasmania, Private Bag 79, Tasmania 7001, Australia*
[c] *Vernadsky Institute of Geochemistry and Analytical Chemistry, Russian Academy of Sciences, 19 Kosygin Str, 119991, Moscow, Russia*
[d] *Research School of Earth Sciences, Australian National University, Canberra, ACT 0200, Australia*
[e] *Grant Institute of Geology, University of Edinburgh, West Mains Road, Edinburgh EH9 3JW, United Kingdom*

Accepted 22 January 2007

Abstract

We have performed a detailed evaluation of three olivine geothermometers for anhydrous systems representing three different approaches to modelling olivine-melt equilibrium. The Ford et al. [Ford, C. E., Russell, D. G., Craven, J.A., Fisk, M. R., 1983. Olivine-liquid equilibria: Temperature, pressure and composition dependence of the crystal/liquid cation partition coefficients for Mg, Fe2+, Ca and Mn. J. Petrol., 24, 256–265.] geothermometer describes olivine liquidus temperature as a function of melt composition and pressure, and the composition of the liquidus olivine as a function of melt composition, pressure and temperature. The Herzberg and O'Hara [Herzberg, C., O'Hara, M.J., 2002. Plume-associated ultramafic magmas of Phanerozoic Age. Journal of Petrology, 43, 1857–1883.] geothermometer describes olivine liquidus temperature similarly to Ford et al. [Ford, C. E., Russell, D. G., Craven, J.A., Fisk, M. R., 1983. Olivine-liquid equilibria: Temperature, pressure and composition dependence of the crystal/liquid cation partition coefficients for Mg, Fe2+, Ca and Mn. J. Petrol., 24, 256–265.], and olivine composition as function of melt composition only. The Putirka [Putirka, K.D., 2005. Mantle potential temperatures at Hawaii, Iceland, and the mid-ocean ridge system, as inferred from olivine phenocrysts: evidence for thermally driven mantle plumes, Geochem. Geophys. Geosyst., 6, Q05L08, doi:10.1029/2005GC000915.] geothermometer describes both olivine liquidus temperature and composition as function of melt composition only. A comparison of these three geothermometers with experimental data at 0.1 MPa and 1.5 GPa reveals that the Ford et al. [Ford, C. E., Russell, D. G., Craven, J.A., Fisk, M. R., 1983. Olivine-liquid equilibria: Temperature, pressure and composition dependence of the crystal/liquid cation partition coefficients for Mg, Fe2+, Ca and Mn. J. Petrol., 24, 256–265.] geothermometer is the most successful in reproducing experimental temperatures and olivine-melt K_D·s. We therefore recommend that the Ford et al. [Ford, C. E., Russell, D. G., Craven, J.A., Fisk, M. R., 1983. Olivine-liquid equilibria: Temperature, pressure and composition dependence of the crystal/liquid cation partition coefficients for Mg, Fe2+, Ca and Mn. J. Petrol., 24, 256–265.] olivine geothermometer be used in parental liquid calculations that involve the incremental addition of olivine to obtain equilibrium with a target olivine phenocryst composition at low pressure. The thermometer of Putirka [Putirka, K.D., 2005. Mantle potential temperatures at Hawaii, Iceland, and the mid-ocean ridge system, as inferred from olivine phenocrysts: evidence for thermally driven mantle plumes, Geochem. Geophys. Geosyst., 6, Q05L08, doi:10.1029/2005GC000915.] was found to systematically

* Corresponding author. Tel.: +61 3 62262270; fax: +61 3 6226 2547.
E-mail address: trevor.falloon@utas.edu.au (T.J. Falloon).

0009-2541/$ - see front matter
doi:10.1016/j.chemgeo.2007.01.015

calculate anomalously high temperatures for high MgO experimental compositions at both 0.1 MPa and 1.5 GPa. The application of the Ford et al. [Ford, C. E., Russell, D. G., Craven, J.A., Fisk, M. R., 1983. Olivine-liquid equilibria: Temperature, pressure and composition dependence of the crystal/liquid cation partition coefficients for Mg, Fe2+, Ca and Mn. J. Petrol., 24, 256–265.] geothermometer to calculate the temperatures of crystallization for parental MORB liquids in mid-crustal magma chambers reveals that there is an ~115 °C temperature range. The hottest MORB parental liquids have crystallisation temperatures of ~1345 °C (MgO contents ~16 wt.%) for a mid-crustal pressure of 0.2 Gpa.

Keywords: Olivine; Geothermometers; Temperature; MORB; Hawaii; Mantle plumes

Contents

1. Introduction

The composition and temperature at which olivine crystallizes from a mantle-derived parental liquid magma at low pressure is one of the key constraints on any model of magma genesis (e.g., Green and Ringwood, 1967; Sobolev and Danyushevsky, 1994), as these parameters are a necessary first step for estimating

potential temperatures of the source mantle. The importance of olivine lies in the fact that it is the first phase to crystallize at low pressure from any mantle-derived melt that is in chemical equilibrium with peridotite and some pyroxenites and eclogites at source depths. This is due to the rapid expansion of the olivine phase volume at lower pressures, demonstrated by numerous experimental studies on model melt compositions. As both olivine crystallisation temperature and the composition of liquidus olivine are highly sensitive to the composition of the crystallising melt, it is possible to calculate both given the composition of melt alone. This is achieved by using empirically calibrated functions for equilibria between melt and olivine end-members. Such a calibration is referred to as an olivine geothermometer (e.g., Roeder and Emslie, 1970).

There exists a large number of olivine geothermometers as well as more simplified empirical formulas for calculating olivine liquidus temperature or composition (e.g., Ford et al., 1983; Nielsen, 1988; Weaver and Langmuir, 1990; Ariskin et al., 1993; Beattie, 1993; Sugawara, 2000; Gudfinnsson and Presnall 2001; Herzberg and O'Hara, 2002; Niu, 2005; Toplis, 2005; Putirka, 2005 and references therein), which often yield contrasting results when applied to natural magmas of various compositions. This is probably because the accuracy of the calculation depends on the experimental data base used for calibration, and the specific form of the compositional dependence used in the model. It follows then that some geothermometers may perform better with some subsets of the natural compositional spectrum. This leads to a necessity to identify the appropriate geothermometer for the task required.

The application of olivine geothermometry to determine the composition of parental liquids is of particular significance to our understanding of the causes of ocean island volcanism (OIB), which are believed to be related to hot mantle plumes. This is because the hypothesis of thermally driven mantle plumes derived from the core–mantle boundary predicts a significant temperature contrast between adiabatically upwelling plume material and ambient upper mantle, especially where there is little or no entrainment between plume materials and ambient upper mantle. Consequently decompression melts derived from the mantle plume materials should be ~200–300 °C hotter than melts derived from ambient upper mantle. However it should be noted that inferred temperature contrasts may well reflect the end-members of possible plume models (Lin and van Keken, 2006). If the thermally driven mantle plume hypothesis is correct then we should expect to find evidence from olivine crystallization temperatures that parental liquids to Hawaii olivine tholeiites, a typical ocean island magma, are significantly hotter than parental liquids to MORB olivine tholeiites. We should also find evidence for very different pressures and degrees of partial melting.

Calculations using various geothermometers have been used to argue both for and against a large contrast between mantle potential temperatures for mid-ocean ridge basalt (MORB) source and ocean island (e.g., Hawaii) basalt source, (e.g., Green and Falloon, 2005; Putirka, 2005). To understand the reasons for these different views, it is important to explore the steps in estimating the crystallization temperature of an olivine crystal in a particular liquid (glass) at a particular pressure (usually at eruption or shallow crustal depth) i.e. applying an olivine geothermometer, and the additional concept of a mantle melting and melt extraction condition, deriving from adiabatic upwelling at a particular mantle potential temperature (McKenzie and Bickle, 1988). One approach uses specific well-documented lavas or suites and a step-by-step approach, i.e. crystallization temperature, parental magma, pressure and temperature of melt segregation, inferred melt fraction and latent heat of melting, and mantle potential temperature (Green et al., 2001 and Green and Falloon, 2005). A second approach (Putirka, 2005) has used large data bases of rock compositions, particularly extending to olivine-rich rocks, to infer that FeO content is a distinctive and characterising variable for magmatic suites and thus for their primary or parental magmas. By selecting a pressure for melt extraction and an olivine composition at the source (residue), a numerical model based on experimental data for olivine-melt equilibria is used to directly infer mantle melting temperature. In this approach the olivine geothermometer is built into the numerical model to yield a single-step calculation from FeO-estimate of primary melt and chosen residual olivine composition and pressure, to yield temperature of mantle melt extraction. The methodology of Putirka (2005) is not a step-by-step approach as used by Green and Falloon (2005) and has the following assumptions: 1) the selected olivine composition (which has crystallized at low pressure) is the same as the olivine in the mantle residue at depth; 2) the pressures of mantle melting are known; 3) the high-pressure K_D·s (defined as $((X_{Fe})^{Ol}/(X_{Fe})^{L})/((X_{Mg})^{Ol}/X_{Mg})^{L})$; where Ol is olivine, L is melt, X_{Fe} and X_{Mg} are cation fractions of Fe^{2+} and Mg, respectively) are known; 4) whole-rock composition which are the result of olivine accumulation can be used to determine FeO contents in primary

or parental compositions and 5) the olivine geothermometer used is well calibrated against relevant experimental data at the pressure of mantle melting.

In contrast to the approach of Putirka (2005) the determination of olivine crystallization temperatures of parental melts at low pressure is the most direct evidence for possible mantle source temperature differences between different suites of basaltic magmas. It is also the first necessary step for estimating mantle potential temperature (Tp). The quantitative calculation of mantle potential temperatures requires estimation or selection of unknowns, such as depth of melt segregation, degree of partial melting, and thermodynamic quantities for the melting reaction (particularly the latent heat of melting). The composition of a parental liquid is also a very important constraint on both forward and inverse models seeking to determine the nature of primary melts and their temperatures of mantle equilibrium. The calculation of olivine crystallization temperatures of parental compositions (as outlined in more detail in Section 2) depends on a choice of an appropriate melt composition including volatile content (preferably glass rather than whole rock), observed olivine phenocryst composition, and an accurate olivine geothermometer. The input data is obtained from naturally occurring erupted magmas and an olivine geothermometer can be chosen which is well calibrated against experimental data at low pressure. If a strong temperature difference does not exist between parental compositions at low pressure, then it is unlikely to exist between their respective mantle sources. This the rationale of Green et al. (2001) and Green and Falloon (2005) in concluding that there is no direct evidence for a large thermal contrast between MORB and Hawaii mantle sources.

Our aim in this study is not to develop or modify the existing olivine geothermometers but to 1) highlight the real differences in performance between olivine geothermometers when calculating parental liquid compositions and 2) to critically evaluate the performance of geothermometers in reproducing experimental temperatures and olivine-liquid K_D.

We critically evaluate (see Section 5) the performance of olivine geothermometers against relevant experimental data. We demonstrate that there are real and significant differences between the ability of different olivine geothermometers to accurately; a) calculate temperatures of olivine crystallization and b) calculate olivine-melt K_D·s in the MgO range of interest. We conclude that the Ford et al. (1983) geothermometer is currently the best at reproducing olivine crystallization temperatures and K_D·s of olivine-melt equilibrium over a wide range of pressures, temperatures and composition. We therefore apply the Ford et al. (1983) geothermometer to estimate crystallization temperatures for parental MORB melts, and show that there exists a range of crystallisation temperatures from ~1230 to ~1345 °C. The higher end of this spectrum is similar to Hawaiian parental melts (ΔT ~6 °C).

2. Estimation of parental magma composition using olivine geothermometers

The use of olivine geothermometers is essential in order to calculate the compositions of parental liquids. This is because unmodified parental liquids rarely erupt, and evidence for their existence is only preserved in the compositions of magnesian olivine phenocrysts observed in more evolved liquid/glass compositions. An olivine geothermometer is therefore used to reconstruct the composition of the parental liquid, and its temperature of crystallisation, by adding back olivine in incremental equilibrium steps (e.g., 0.01 wt.%, see appendix in Danyushevsky et al., 2000 for a detailed explanation) into an evolved liquid composition. This use of an olivine geothermometer assumes that olivine crystallises fractionally, i.e. olivine is chemically isolated from the melt when it is formed. Evidence for widespread fractional crystallization of olivine from mantle-derived magmas is presented by Danyushevsky et al. (2002). If however olivine crystallizes partly by equilibrium crystallization (that is some proportion of olivine phenocrysts remains in the magma and changes composition as the magma cools), then the assumption of fractional crystallization will cause olivine crystallization temperatures to be underestimated depending on the ratio of fractional to equilibrium crystallization (calculations using PETROLOG software, Danyushevsky, 2001, indicate that this error is ~6 °C for a 50:50 ratio of equilibrium to fractional crystallization, for tholeiite parental liquids of ~15 wt.% MgO). As well as the assumption of fractional crystallization, the parental liquid calculation also requires the following:

2.1. A composition of an evolved melt within the olivine-only field

This should be either a natural glass composition or an aphyric whole-rock composition which represents a liquid. With regard to this requirement, clarity in the use of the word ‘magma’ is also required as it is not uncommon to find publications in which observed ‘picrite magma’ is equated with high temperature melts whereas many picrites are accumulates in which

olivine has been concentrated by crystal settling (see Danyushevsky et al., 2002 for a detailed discussion on the origin of olivine-phyric volcanic rocks). In such rocks it is the glass (or aphyric groundmass) and olivine microphenocrysts or phenocryst rims which contain evidence for the temperature at quenching (and not the bulk composition). Careful documentation of more magnesian phenocryst cores is required to argue for more olivine-rich and higher temperature parental melt composition. In this paper we endeavour to maintain clarity between the use of 'magma' which may include crystals, liquid and vapour phases within the mobile magma body and 'melt' or 'liquid' referring to both a single phase and its composition.

2.2. To establish the composition of the most magnesian olivine phenocryst or microphenocryst for the suite, as a target for the olivine addition calculations

In any magma suite there will be found a range in olivine phenocryst compositions (Danyushevsky et al., 2002). Most large olivine phenocrysts show normal zoning from core Mg# values higher than the olivine compositions in equilibrium with the erupted evolved liquid composition. Olivine in equilibrium with the erupted melt is usually present as both discrete microphenocrysts and rims on the more magnesian phenocryst cores. In some suites the magnesian olivine phenocrysts are xenocrystic and could either represent 1) disaggregated cumulate material from previously erupted magmas, which may or may not have similar magma compositions to the composition of interest or 2) lithospheric wall rock samples ripped off and disaggregated as magmas or melts have moved through the lithosphere towards crustal magma chambers. However in most suites it is possible to identify and analyse melt inclusions in magnesian olivine phenocrysts which demonstrate that these olivine phenocrysts are related to the evolved liquid composition which has erupted, via the process of crystal fractionation. Minor element or trace element contents of olivine may also be used to discriminate phenocryst vs xenocryst relationship to the host magma. For phenocryst and microphenocryst relationships, it is possible to use an olivine geothermometer to incrementally add back olivine in small equilibrium steps to obtain a parental composition that is in equilibrium with the most magnesian phenocryst composition observed (Irvine, 1977; Albarede, 1992; Danyushevsky et al., 2000). What is important is that some justification needs to be given for the choice of a target olivine composition. Consideration should also be given to the possibility of sampling error, and the potential role of equilibrium crystallization (i.e. the maximum observed magnesian phenocryst may have already changed its composition as the magma cooled, e.g., Gaetani and Watson, 2002). The choice of the target olivine is a critical input parameter as a change in 1 mol% Fo in olivine can potentially lead to differences of between 30–60 °C depending on the model olivine geothermometer used.

2.3. An estimate of volatile content of the evolving melt (especially H_2O) and its effect on the crystallisation temperature and composition

The use of anhydrous calculations for magmas with small amounts of H_2O can lead to significant differences in calculated crystallization temperatures (e.g.,Falloon and Danyushevsky, 2000). In this paper we use the model of Falloon and Danyushevsky (2000) to estimate the effect of H_2O, on olivine liquidus temperatures. The model of Falloon and Danyushevsky (2000) predicts a liquidus depression of ~60 °C for 0.6 wt.% H_2O in the melt. The effect of H_2O on the value of the equilibrium constant for iron-magnesium exchange between olivine and liquid (K_D) is less well-known but experimental and theoretical studies (Ulmer, 1989; Toplis, 2005; Putirka, 2005) suggest that the effect is very small for the likely H_2O contents of tholeiite parental liquids (<1 wt.%) and will not introduce a significant error into calculations by olivine geothermometers under anhydrous conditions. As other C–H–O volatiles (e.g., CO_2, CH_4) have significantly lower solubilities in the melt phase at low pressures compared to H_2O their negligible effect on the olivine liquidus surface has not been taken into account in this approach. However the effect of C–H–O volatiles cannot be ignored for calculations performed at higher pressures where solubilities in the melt can become significant (Taylor and Green, 1987; Gudfinnsson and Presnall, 2005).

2.4. An estimate of melt oxidation state

Two components are necessary, i) an oxygen fugacity and ii) a model to calculate the Fe^{3+}/Fe^{2+} ratio of the melt for the given oxygen fugacity (see Danyushevsky and Sobolev, 1996; Nikolaev et al., 1996 for a detailed discussion). Differences in oxygen fugacity will not have a serious effect on conclusions reached about temperature differences between parental compositions (~40 °C for four orders of

magnitude difference in the oxygen fugacity, QFI versus Ni–NiO buffers, see also Kägi et al., 2005 who demonstrate a 25 °C difference for three orders of magnitude in oxygen fugacity).

2.5. An estimate of pressure for crystallisation of the olivine phenocrysts

This can be determined from studies of primary fluid inclusions in olivine phenocrysts (e.g., Anderson and Brown, 1993; Sobolev and Nikogosian, 1994).

2.6. An appropriate olivine geothermometer

In this paper we will argue that for the purposes of calculating parental compositions at low pressure (to 3–4 GPa) the Ford et al. (1983) model is the most appropriate olivine geothermometer to use as it can most accurately recover experimental olivine-melt K_D·s (see discussion below).

3. Comparison between formulations of different olivine geothermometers

Olivine geothermometers are not all in agreement with respect to temperature calculations. As geothermometers provide both olivine composition and temperature, differences in formulation results in models giving agreement in temperature, but not composition, or vice versa (see some representative examples below, Section 4). Roeder and Emslie (1970) were the first to publish a model at 0.1 MPa. In the Roeder and Emslie (1970) model, K_D is essentially independent of temperature and melt composition, with a value of ~0.3. This was important for petrology as if the value of the K_D is known the composition of olivine can be calculated from the melt composition. Therefore with a known value of K_D, it is possible to calculate a parental composition given a target olivine composition, by simply using a single K_D value (e.g., Eggins, 1993). The Roeder and Emslie (1970) study leads to the commonly accepted view that the K_D value of 0.3 could be applied in a wide range of melt generation models, including olivine addition calculations.

However subsequent experimental work at pressures >0.1 MPa has demonstrated higher K_D values, and it was assumed that this difference was due to effect of pressure on K_D (e.g. Takahashi and Kushiro, 1983). With increase in the number of available experimental data it became apparent that the higher K_D values in high-pressure experiments are mainly due to the effect of temperature (Sobolev and Danyushevsky, 1994), and the effect of pressure is small and essentially negligible. The initial interpretations of a pressure effect on K_D resulted simply because most higher pressure experiments are conducted at higher temperatures and in general, the higher the pressure of the experiment, the higher is the associated temperature.

There are two important factors making up the K_D–temperature relationship. The first is related to changes in melt composition. Increasing the amount of olivine component in the melt leads to a higher liquidus temperature, and the K_D value can thus be tied to the melt composition (e.g., Beattie, 1993). As well experiments on olivine-melt equilibria on different melt compositions (from alkaline to komatiites), since the study of Roeder and Emslie (1970) have shown that even at 0.1 MPa, K_D is a function of melt composition, mainly alkalies and TiO_2 (e.g. Takahashi,1978). The second component is not related to composition but is directly related to the well-established effect of pressure on the olivine liquidus temperature (Davis and England, 1964). The effect of pressure is ~50 °C/GPa, i.e. if a composition is within the olivine stability field over a range of pressures, then there should be a range of olivine liquidus temperatures and olivine composition.

There are potentially a large choice of olivine geothermometers or empirical calibrations which could have been evaluated herein (e.g. Roeder and Emslie, 1970; Ford et al., 1983; Sobolev and Slutsky, 1984; Nielsen, 1985; Ariskin et al., 1987; Nielsen, 1988; Weaver and Langmuir, 1990; Langmuir et al., 1992; Ariskin et al., 1993; Beattie, 1993; Sugawara, 2000; Danyushevsky, 2001; Herzberg and O'Hara, 2002; Putirka, 2005; Toplis 2005). For our comparison we have chosen three representative geothermometers which treat the temperature–composition relationship differently. Two of these, Ford et al. (1983) and Herzberg and O'Hara (2002) are representative of the performance of all previously published geothermometers, whereas the third, Putirka (2005), is unique and gives a different result from the other two geothermometers.

The model of Ford et al. (1983) describes olivine liquidus temperature as a function of melt composition and pressure, and the composition of liquidus olivine as a function of melt composition, temperature and pressure. Thus the Ford et al. (1983) model will calculate different olivine composition in equilibrium with the same melt at low and high pressures. The model of Herzberg and O'Hara (2002) describes olivine liquidus temperature similarly to Ford et al. (1983), but olivine composition is a function of melt composition only. Thus the Herzberg and O'Hara (2002) model

will calculate the same olivine composition in equilibrium with the same melt at low and high pressure. The Putirka (2005) model describes both olivine liquidus temperature and composition as a function of melt composition only. Thus the Putirka (2005) model will calculate only one temperature and composition for a given melt regardless of pressure.

A large number of existing models only work at 0.1 MPa and thus were not included in this comparison. Among the models which can work at higher pressure, a similar approach to Ford et al. (1983) is used in COMAGMAT (see Ariskin and Barmina, 2004 for discussion) and Langmuir et al. (1992) models. The formulation of Beattie (1993) is used by the Herzberg and O'Hara (2002) model and hence Herzberg and O'Hara (2002) is the most recent model which uses this approach. In order to successfully perform olivine addition calculations a geothermometer needs to be able to calculate both temperature and K_D at each equilibrium incremental step. We have not, therefore evaluated the recent K_D model of Toplis (2005) as this model requires temperature as an input in order to calculate K_D. Thus the Toplis (2005) model can only be used in combination with another olivine geothermometer in order to perform olivine addition calculations.

4. Why is a choice of an olivine geothermometer important?

The answer to the above question is discussed with reference to the results of incremental olivine addition calculations on two natural glass compositions (Table 1) presented in Tables 2 and 3. Two different sets of calculations are presented in Tables 2 and 3 which both demonstrate how the choice of olivine geothermometer and/or the olivine-liquid K_D can produce different results. In Table 2 calculations are presented which demonstrate the outcomes resulting from different choices to determine crystallization temperatures of parental compositions at low pressure. The examples selected in Table 2 aim to compare Hawaiian and MOR picrites. In Table 3 calculations are presented which demonstrate how a similar range in choices can result in significant differences in the calculated parental composition and temperature of crystallization for a single MORB glass composition.

Table 1
Primitive glass compositions used in parental melt calculations presented in Table (2)

	MORB	Hawaii
	896A 27r-1, pc. 15	57–13 g
SiO_2	49.03	48.3
TiO_2	0.64	1.88
Al_2O_3	16.07	10.9
FeO	9.12	11.8
MnO	0.12	nd
MgO	9.43	14.8
CaO	13.66	8.6
Na_2O	1.62	1.62
K_2O	0.02	0.32
P_2O_5	0.03	0.19
H_2O	0.05	0.57
Oliv (Mg#)	91.6	90.7

Data sources: MORB, McNeill and Danyushevsky (1996); Hawaii, Clague et al. (1995).

4.1. Temperature differences between MORB and Hawaii parental compositions

Although disagreement over the differences in crystallization temperatures could in part be attributed to the differences in choice of liquid/olivine compositions and a range of intensive parameters (e.g. oxygen fugacities, volatile contents, pressure of crystallization), the main cause of difference is the choice of olivine geothermometer and/or the olivine-liquid K_D (used in calculating parental magma compositions). This is illustrated in Tables 1 and 2. Table 1 presents two primitive glass compositions, one each from MORB and Hawaiian settings. Both glasses are natural examples containing olivine microphenocrysts with a range of core compositions, extending to Mg# [Mg# = 100 * (X_{Mg}/(X_{Mg} + X_{Fe})] 91.6 in the case of the MORB sample and 90.7 in the case of the Hawaiian sample. In Table 2, we present the results of calculations at 0.1 MPa using three different olivine geothermometers in the form of a grid, showing the range of $\Delta T = T^{Hawaii} - T^{MOR}$ values obtained between calculated parental compositions. The results of two different calculations are summarized in Table 2.

In the first type of calculation, both olivine composition and K_D are derived from the 'olivine thermometer' formulation. Olivine is incrementally added back into the glass compositions in steps of 0.01 wt.% until equilibrium with the target olivine composition is achieved. The target olivine for the MORB composition is Mg# 91.6 and for the Hawaiian composition the target olivine is Mg# 90.7. Both olivine targets are the maximum Mg# observed as phenocrysts (in both cases microphenocrysts) in the natural sample. In each step the equilibrium olivine is calculated by the olivine

Table 2
Temperature difference grid between calculated parental melts for Hawaii (top row, across) and MORB (left hand side, down) using a range of different olivine geothermometers and olivine-liquid K_D·s at 0.1 MPa (see text for discussion)

		HAWAII (target oliv 90.7)								
		0.31 F^1	HO^1 0.34	P^1 0.34	0.32 F^2	0.32 HO^2	0.32 P^2	0.38 F^2	0.38 HO^2	0.38 P^2
		1342	1376	1521	1349	1356	1461	1396	1406	1525
MORB (target oliv 91.6)										
0.30 F^1	1336	**6**	40	185	13	20	125	60	70	189
0.34 HO^1	1371	−29	**5**	150	−22	−15	90	25	35	154
0.33 P^1	1459	−117	−83	**62**	−110	−103	2	−63	−53	66
0.32 F^2	1360	−18	16	161	**−11**	−4	101	36	46	165
0.32 HO^2	1353	−11	23	168	−4	**3**	108	43	53	172
0.32 P^2	1425	−83	−49	96	−76	−69	**36**	−29	−19	100
0.38 F^2	1421	−79	−45	100	−72	−65	40	**−25**	−15	104
0.38 HO^2	1416	−74	−40	105	−67	−60	45	−20	**−10**	109
0.38 P^2	1510	−168	−134	11	−161	−154	−49	−114	−104	**15**

Olivine geothermometers as follows: F, Ford et al. (1983); HO, Herzberg and O'Hara (2002); P, Putirka (2005) models C & D. Superscripts 1 and 2, refer to calculation method 1 and method 2 respectively (see text for discussion). K_D·s used are indicated beside the appropriate geothermometer (see text for discussion), for example "0.32 F^2" refers to a model calculation using a fixed K_D of 0.32 with temperature calculated using the geothermometer of Ford et al. (1983), whereas "0.30 F^1" refers to a model calculation in which K_D is calculated by the Ford et al. (1983) olivine geothermometer, with a final calculated K_D of 0.3 in equilibrium with the target olivine of 91.6. MORB and Hawaii glass compositions used in the calculations are presented in Table 1. All MORB calculations were done at an oxygen fugacity of QFM−0.5 log units and for Hawaii QFM+0.5 log units. Fe_2O_3 contents were calculated using the model of Borisov and Shapkin (1990). Olivine liquidus depression due to H_2O was calculated using the empirical model of Falloon and Danyushevsky (2000) for the Ford et al. (1983) and the Herzberg and O'Hara (2002) geothermometers. H_2O contents used are listed in Table 1. All calculations were performed using the software PETROLOG (Danyushevsky, 2001).

geothermometer, that is the resulting K_D is determined by the olivine geothermometer. The results of these calculations of crystallisation temperature are indicated by the letters "0.30 F^1" (Ford et al., 1983 geothermometer), "0.34 HO^1" (Herzberg and O'Hara, 2002 geothermometer) and "0.33 P^1" (Putirka, 2005 geothermometer) in Table 2. The numbers refer to the final equilibrium K_D value calculated by the respective geothermometer.

In the second type of calculation, the equilibrium olivine at each incremental step is calculated not by the olivine geothermometer but by using an imposed constant K_D value. Two examples are given for K_D values of 0.32 and 0.38 for all three geothermometers (results indicated by abbreviations "0.32 F^2" etc).

The resulting ΔT values are coded in Table 2. Heavy shaded areas are ΔT values ≥ 70 °C, light shaded areas ΔT values ≤ -70 °C and areas of no shading are ΔT values lying between −70 °C and 70 °C. Thus depending on the combination of olivine geothermometer used, the K_D values selected Hawaii could be either up to ~189 °C hotter or ~168 °C colder than MORB. If the same combination of model and calculation technique is applied to both the MORB and Hawaiian compositions then ΔT ($T^{Hawaii} - T^{MOR}$) values have a more restricted range from 62 °C to −25 °C (bold numbers in diagonal table cells). It is clear from Table 2, that olivine crystallization temperatures could be used to both support or refute the thermally driven mantle plume hypothesis, and therefore the choice of olivine geothermometer and/or K_D is of primary importance.

4.2. Differences between calculated parental compositions for a single MORB glass composition

In Table 3 we have taken the primitive MORB glass composition from Table 1 and calculated

Table 3
Calculated parental compositions in equilibrium with olivine Mg# 91.6, using a range of olivine geothermometers and K_D·s

	Ford et al (1983)			Herzberg and O'Hara (2002)		Putirka (2005)		Constant K_D	
	0.1 MPa	0.1 MPa[a]	1 GPa	0.1 MPa	1 GPa	0.1 MPa	1 GPa	(a)	(b)
SiO_2	47.76	48.03	47.44	47.23	47.33	47.51	47.51	47.98	46.70
TiO_2	0.54	0.56	0.52	0.51	0.51	0.52	0.52	0.56	0.46
Al_2O_3	13.57	14.07	13.00	12.65	12.84	13.13	13.13	13.98	11.62
Fe_2O_3	0.81	0.76	1.08	0.88	1.07	1.29	1.29	0.76	1.07
FeO	8.58	8.54	8.45	8.57	8.37	8.18	8.18	8.54	8.69
MnO	0.1	0.11	0.1	0.12	0.12	0.1	0.1	0.1	0.09
MgO	15.59	14.42	16.93	17.83	17.37	16.64	16.64	14.63	20.20
CaO	11.54	11.96	11.05	10.80	10.95	11.16	11.16	11.88	9.88
Na_2O	1.37	1.42	1.31	1.27	1.29	1.32	1.32	1.41	1.17
K_2O	0.02	0.02	0.02	0.02	0.02	0.02	0.02	0.02	0.01
P_2O_5	0.03	0.03	0.02	0.02	0.02	0.02	0.02	0.03	0.02
K_D	0.297	0.276	0.327	0.34	0.34	0.332	0.332	0.28	0.38
% Oliv added	15.6	12.5	19.1	21.5	20.3	18.3	18.3	13.1	27.7
T (°C)	1336	1312	1412	1371	1415	1459	1459		
T (°C)$_F$								1316	1421
T (°C)$_{HO}$								1309	1416
T (°C)$_P$								1363	1510

All calculations were performed using the software PETROLOG (Danyushevsky, 2001). Calculations were performed at an oxygen fugacity of QFM−0.5 log units, and Fe_2O_3 contents were calculated using the model of Borisov and Shapkin (1990). The effect of the small amount of H_2O in the MORB melt (0.05 wt.%, Table 1) on olivine liquidus temperature is calculated using the model of Falloon and Danyushevsky (2000), except Putirka (2005) which calculates a liquid depression as part of model C and D of Putirka (2005). Olivine was added incrementally in steps of 0.01 wt.%. Subscript abbreviations F, HO and P refer to the geothermometers used to calculated temperature in the case of using a constant K_D, F=Ford et al. (1983), HO = Herzberg and O'Hara (2002), and P = Putirka (2005). K_D refers to the final calculated equilibrium value when the melt is calculated to be in equilibrium with olivine of Mg# 91.6. 0.1 MPa[a] refers to a model calculation using the Ford et al. (1983) geothermometer to calculate temperature and the Toplis (2005) model to calculate K_D.

parental liquid compositions in equilibrium with olivine of Mg# 91.6 using our three representative olivine geothermometers and using the software PETROLOG (Danyushevsky, 2001). We have performed the calculations at both 0.1 MPa and 1 GPa. For each calculation at 0.1 MPa and 1 GPa the final equilibrium K_D calculated by the respective olivine geothermometer is listed in Table 3. As parental composition can also be calculated using a fixed K_D value, for comparison we also present calculations using a fixed K_D value of 0.28 and 0.38. These K_D values were chosen as they encompass the range in most experimental K_D·s at 0.1 MPa (see Section 5 and Fig. 4 below). In this case the liquidus of the inferred parent liquid is calculated separately using each olivine geothermometer ("T (°C)$_F$" etc, see Table 3).

Table 3 demonstrates that the calculated parental melt compositions for the MORB glass varies in MgO from ~14 to 20 wt.%, and calculated equilibrium temperatures vary from 1309 to 1510 °C, a very significant range. Using Table 3, we discuss the different performances of the three representative olivine geothermometers.

4.2.1. Ford et al. (1983)

The results for the Ford et al. (1983) geothermometer (Table 3) show that it calculates a parental liquid of 15.59 wt.% MgO, 1336 °C, with a final K_D of 0.297 at 0.1 MPa and at 1 GPa a parental liquid of 16.93 wt.% MgO, 1412 °C with a final K_D of 0.327 (Table 3). The differences between the two calculations arise because the K_D is calculated as a function of composition, pressure and temperature. Thus as pressure increases, the Ford et al. (1983) model will calculate higher K_D·s, which is consistent with experimental data which demonstrates that K_D increases with pressure (due to higher temperatures). Therefore depending on pressure, the use of the Ford et al. (1983) model will result in a different parental composition for a fixed target olivine composition, or alternatively different equilibrium olivine compositions for a fixed parental composition (high-pressure equilibrium olivine composition is less magnesian

Table 4
Statistical analysis of calculated olivine liquidus temperatures and K_D versus experimental temperatures and K_D

Geothermometer	Ford et al. (1983)		Herzberg and O'Hara (2002)		Putirka (2005)	
	Temperature	K_D	Temperature	K_D	Temperature	K_D
Grove and Bryan (1983)						
r	0.9297	0.5756	0.9225	−0.3589	0.8891	−0.1027
s.e.	3.4	0.001	4.7	0.004	2.8	0.012
Slope (a)	0.9932	0.3798	0.9535	−0.172	1.1004	−0.0223
Δ (T, K_D)	8±4	0.012±0.004	9±4	0.019±0.007	14±7	0.012±0.001
Montierth et al. (1995)						
r	0.9928	−0.2441	0.9943	0.4794	0.9850	0.5394
s.e.	13.2	0.006	12.5	0.028	31.3	0.013
Slope (a)	1.0482	−0.0697	1.1081	0.5804	1.7199	0.4128
Δ(T, K_D)	5±1	0.011±0.001	7±6	0.024±0.027	44±67	0.014±0.013
0.1 MPa>9 wt.% MgO						
r	0.9376	0.6034	0.9593	0.1603	0.8844	0.5296
s.e.	2.8	0.008	4.0	0.004	10.8	0.004
Slope (a)	0.8399	0.3493	0.9215	0.0416	1.4633	0.2829
Δ(T, K_D)	16±8	0.024±0.020	13±1	0.038±0.013	51±5	0.028±0.014
1.5 Gpa						
r	0.9752	0.6341	0.9836	0.7568	0.9691	0.7114
s.e.	19.0	0.022	18.0	0.012	48.0	0.022
Slope (a)	0.861	0.5275	0.9727	0.5727	1.9292	0.5061
Δ(T, K_D)	18±27	0.025±0.021	12±15	0.016±0.012	85±2	0.019±0.019

r is the pearson correlation coefficient between calculated and experimental temperatures or K_D·s; s.e. standard error of estimation; Slope (a), the slope of linear regression ($Y_{calculated}=a*X_{experimental}+b$); $\Delta(T, K_D)=(T, K_D)_{experimental}-|(T, K_D)_{calculated}|$, ± refers to 1 standard deviation. Data sources for 0.1 MPa>9 wt.% MgO experiments as follows: Ford et al. (1983) ($n=68$, see Appendix A); Murck and Campbell (1986) $n=19$; Walker et al. (1988), $n=7$; Parman et al. (1997), $n=12$; Sack et al. (1987), $n=3$; Montierth et al. (1995), $n=5$; Grove and Bryan (1983), $n=9$; Arndt (1977), $n=3$; Boivin (1980), $n=6$; Grove (1981), $n=4$; Grove et al. (1982), $n=2$; Walker et al. (1976), $n=2$; Longhi et al. (1978), $n=7$; Bender et al. (1978), $n=8$; Huebner et al. (1976), $n=6$; Rhodes et al. (1979), $n=6$; Akella et al. (1976), $n=9$; Longhi and Pan (1988), $n=14$).

than low-pressure equilibrium olivine composition). For example the 0.1 MPa calculated parental composition is in equilibrium with olivine of Mg# 91.6, but at 2 GPa the same composition is in equilibrium with olivine of Mg# 90.1 at a temperature of 1438 °C according to the Ford et al. (1983) model.

As a comparison with the Ford et al. (1983) model we also present a calculation at 0.1 MPa using the model of Toplis (2005) to calculate K_D, with temperature calculated using the Ford et al. (1983) model. Note that the Toplis (2005) model calculates significantly lower K_D·s at 0.1 MPa than the other three models.

4.2.2. Herzberg and O'Hara (2002)

The results for the Herzberg and O'Hara (2002) geothermometer (Table 3) show that it calculates a parental liquid of almost identical composition at both 0.1 MPa and 1 GPa (slight differences are due to the temperature and pressure effects on oxygen fugacity at the reference buffer chosen). This is because in the Herzberg and O'Hara (2002) model K_D is a function of melt composition only, and hence identical K_D values are used in each incremental step at 0.1 MPa and 1 GPa to calculate the parental composition. This also results in the same equilibrium olivine composition regardless of the pressure of crystallization. The Herzberg and O'Hara (2002) model calculates (as does the Ford et al., 1983 geothermometer) a higher olivine liquidus temperature at 1 GPa due to the well-known increase in olivine liquidus temperatures with pressure (~5 °C / 0.1 GPa; 4.77 °C for the simple system MgO–SiO_2, Davis and England, 1964).

4.2.3. Putirka (2005)

The results for the Putirka (2005) geothermometer (Table 3) show that, like that the Herzberg and O'Hara (2002) geothermometer, it calculates a parental liquid of identical composition at both 0.1 MPa and 1 GPa. The

Putirka (2005) geothermometer also calculates an identical crystallization temperature for both 0.1 MPa and 1 GPa. Both these results are due to the fact that the Putirka (2005) geothermometer does not take into account the effect of pressure on both K_D and olivine liquidus temperature. Note the temperatures of olivine crystallization for the parental MORB compositions is 123 °C higher than for the Ford et al. (1983) geothermometer at 0.1 MPa.

4.2.4. Constant K_D

The calculations using constant K_D (Table 3, using K_D of 0.28 and 0.38) reveal significant differences in calculated olivine crystallization temperatures between the Putirka (2005) geothermometer [$(T/°C)_P$] and the other two geothermometers. With a K_D of 0.28 the Putirka (2005) is 54 °C higher and with a K_D of 0.38, it is 94 °C higher than the Herzberg and O'Hara (2002) geothermometer.

4.3. Summary — the choice of olivine geothermometer is important

The maximum temperature difference observed in the model calculations presented in Table 3 is 201 °C (Putirka, 2005 at a K_D of 0.38 versus Herzberg and O'Hara, 2002 at a K_D of 0.28). This difference is in the same order as what is expected for the temperature differences between mantle plumes and ambient upper mantle. The results from Table 3 demonstrate how it is possible using a combination of geothermometers and assumed K_D to generate the results presented in Table 2. Without a critical evaluation of olivine geothermometers used it is possible to create either an argument for MORB parental liquids to be hotter, the same or colder than Hawaiian parental liquids. Green et al. (2001) and Green and Falloon (2005) argue for no significant temperature differences between the parental compositions of MORB and Hawaii at low pressure using the Ford et al. (1983) geothermometer. In order to resolve this large potential range in calculated crystallization temperatures of parental liquids it is necessary to critically evaluate olivine geothermometers against experimental data to determine which geothermometer gives the most reliable calculations of olivine crystallization temperatures.

5. Critical evaluation of the representative olivine geothermometers

In order to evaluate the olivine geothermometers we have tested them against four experimental databases. The databases used are as follows: 1) The experimental study of Grove and Bryan (1983) on a range of MORB glass compositions at controlled oxygen fugacity at 0.1 MPa (number of experiments = 37); 2) The experimental study of Montierth et al. (1995) on a range of Mauna Loa tholeiite compositions from Hawaii at controlled oxygen fugacity at 0.1 MPa (number of experiments = 12); 3) A database of 190 experimental olivine-melt compositions at 0.1 MPa under controlled oxygen fugacity (a subset of the data is presented in Appendix A). Importantly the melt compositions all have MgO contents >9 wt.% MgO and encompasses the range of MgO contents (data range 9–25 wt.%) expected during incremental olivine addition to calculate parental liquid compositions for both MORB and Hawaiian tholeiite magmas. We could have chosen a very large experimental database at 0.1 MPa to evaluate the three geothermometers (for example the Ford et al., 1983, database alone consists of 747 experiments), but what is critical is the ability of the olivine thermometers to reproduce temperatures and K_D·s in the MgO range in which the olivine addition calculations are performed. A geothermometer may be quite accurate for compositions with MgO <9 wt.%, which is appropriate for most terrestrial glasses and aphyric magmas, but perform poorly at higher MgO contents; and 4) a database of 55 olivine-melt compositions at 1.5 GPa from a selection of published and new peridotite melting and peridotite-reaction experiments (presented in Appendix B). An evaluation of the olivine geothermometers against a high-pressure data set is important, as olivine crystallization temperatures are used as a basis for estimation of mantle potential temperatures. The calculation of mantle potential temperatures among other parameters requires at some point a calculation of a temperature of equilibrium with an upper mantle olivine-bearing residue. Thus the olivine geothermometers must also be able to predict temperatures at high pressures for olivine-melt equilibria.

The results of our evaluation are presented in Table 4 and Figs. 1–6. We evaluated the ability of the geothermometers to reproduce both experimental temperature and K_D. In all 0.1 MPa experiments the Fe^{3+}/Fe^{2+} ratio in the melt at the corresponding reported experimental oxygen fugacity was calculated using the model of Borisov and Shapkin (1990). As the 1.5 GPa experiments were all run in graphite capsules, all Fe in the melt is assumed to be Fe^{2+}, for the purposes of calculating experimental K_D·s. However we note that a small error may be introduced into our calculations for lower temperature

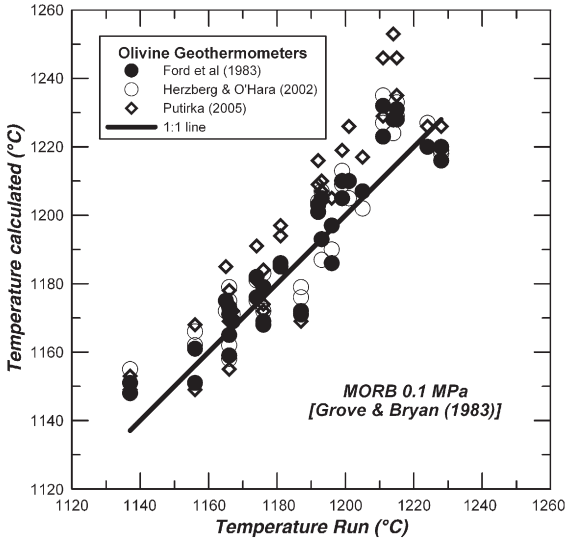

Fig. 1. Experimental run temperatures versus calculated run temperatures from the study of Grove and Bryan (1983) using the Ford et al. (1983), Herzberg and O'Hara (2002) and the Putirka (2005) olivine geothermometers.

runs (<1300 °C, $n=2$, Appendix B) at 1.5 GPa, as both Ulmer and Luth (1991) and Frost and Wood (1995) suggest that the oxygen fugacity on the graphite–CO fluid surface is around wustite–magnetite or Co–CoO, and thus for these experiments there could be a small but undetermined amount of Fe^{3+} present. We also used both of the composition dependent models C and D of Putirka (2005) in all calculations.

5.1. Grove and Bryan (1983) — MORB database

The study of Grove and Bryan (1983) provides a dataset of coexisting olivine-melt compositions appropriate for MORB compositions. With regards to MORB compositions at 0.1 MPa the Ford et al. (1983) geothermometer has been previously evaluated in the study of Danyushevsky et al. (1996). Danyushevsky et al. (1996) evaluated the Ford et al. (1983) model along with three other olivine geothermometers (Roeder and Emslie, 1970; Ariskin et al., 1987; Weaver and Langmuir, 1990) using a database consisting of 69 0.1 MPa MORB experiments (in all experiments both olivine and plagioclase were present and MgO ≥ 5.5 wt.%). Danyushevsky et al. (1996) found the Ford et al. (1983) the best performing geothermometer of these four.

The results of our evaluation of the three representative geothermometers are presented in Table 4 and Fig. 1. As can be seen from Table 4 and Fig. 1, in terms of temperature, both the Ford et al. (1983) and Herzberg and O'Hara (2002) geothermometers are equally as good at reproducing experimental

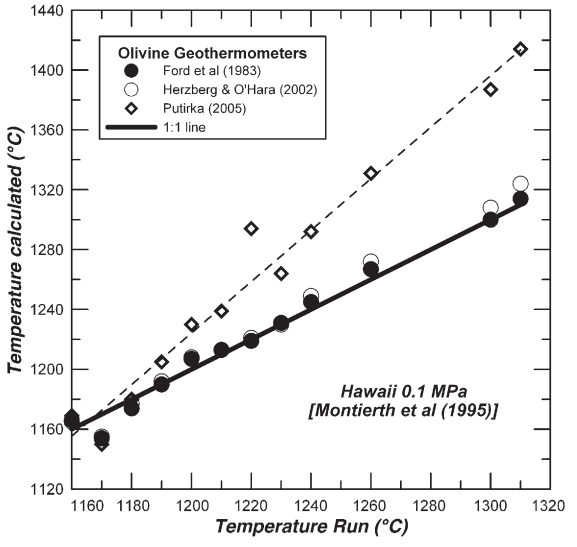

Fig. 2. Experimental run temperatures versus calculated run temperatures from the study of Montierth et al. (1995) using the Ford et al. (1983), Herzberg and O'Hara (2002) and the Putirka (2005) olivine geothermometers. Thin line is a linear regression through the Putirka (2005) calculations.

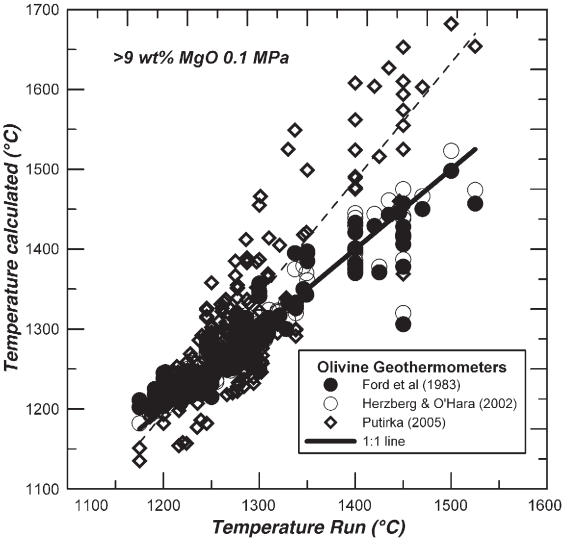

Fig. 3. Experimental run temperatures versus calculated run temperatures for 190 olivine-liquid experimental compositions in which MgO is >9 wt.% in the co-existing liquid (see text for discussion, data as for Table 4) using the Ford et al. (1983), Herzberg and O'Hara (2002) and the Putirka (2005) olivine geothermometers. Thin line is a linear regression through the Putirka (2005) calculations.

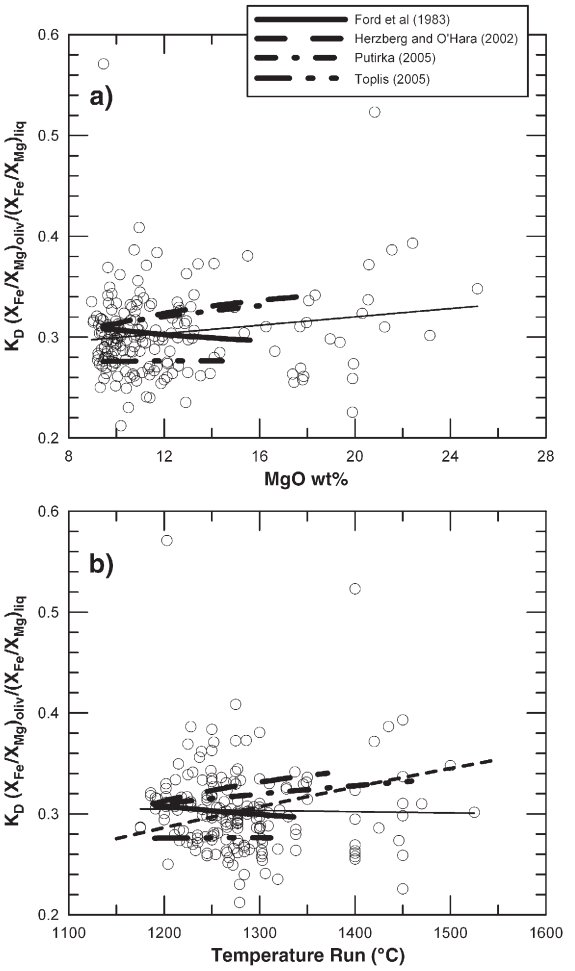

Fig. 4. Olivine-melt K_D·s plotted against MgO wt.% (a) and experimental temperature (b) for 190 olivine-liquid experimental compositions in which MgO is >9 wt.% in the co-existing liquid (see text for discussion). Thin line in both (a) and (b) is a linear regression through for the entire data set. In both (a) and (b) we show the trends of calculated K_D for the three geothermometers and the K_D model of Toplis (2005) which resulted in the calculated parental liquid compositions at 0.1 MPa presented in Table 3. Heavy dashed line in (b) is the variation of K_D with temperature predicted by the model of Sobolev and Danyushevsky (1994).

temperatures, and superior to the Putirka (2005) model. The Putirka (2005) model in some cases, especially at higher MgO contents, calculates significantly higher temperatures than the other two geothermometers (max difference 29 °C). In terms of K_D, Table 4 shows that the Ford et al. (1983) model is the most accurate in reproducing experimental K_D·s, although in general none of the geothermometers can reproduce experimental K_D·s as well as experimental temperatures.

5.2. Montierth et al. (1995) — Hawaiian database

The study of Montierth et al. (1995) provides a dataset of coexisting olivine-melt compositions appropriate for Hawaiian tholeiite compositions. The results of our evaluation are presented in Table 4 and Fig. 2. As can be seen from Table 4 and Fig. 2, both the Ford et al. (1983) and Herzberg and O'Hara (2002) models are equally as good at reproducing experimental temperatures and clearly superior to the model of Putirka (2005) which displays a systematic deviation towards higher calculated temperatures with increasing MgO content (i.e. higher run temperatures, see Fig. 2). The maximum difference calculated between the Putirka

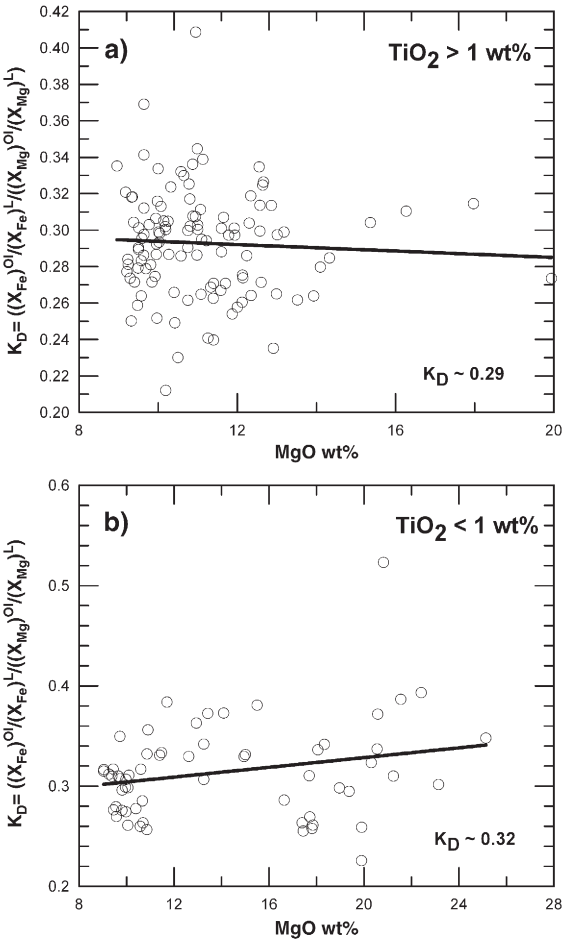

Fig. 5. Olivine-melt K_D·s plotted against MgO wt.% in the liquid for 190 olivine-liquid experimental compositions in which MgO is >9 wt.% in the co-existing liquid (see text for discussion). Data as for Table 4. In a) liquid compositions in which TiO_2 > 1 wt.% are plotted whereas in b) has liquid compositions in which TiO_2 < 1 wt.%. Solid lines in both a) and b) are linear regressions through the data.

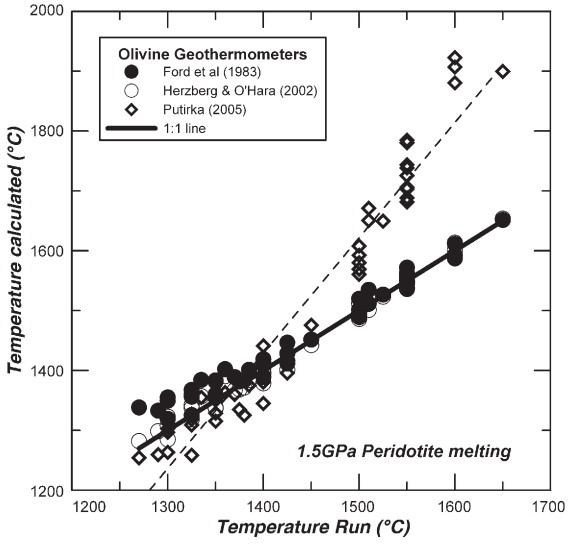

Fig. 6. Experimental run temperatures versus calculated run temperatures for 55 1.5 GPa peridotite melting and reaction experiments (Appendix A) using the Ford et al. (1983), Herzberg and O'Hara (2002) and the Putirka (2005) olivine geothermometers. Dotted line is a linear regression through the calculated data of Putirka (2005).

(2005) and the other two geothermometers is 100 °C. In terms of K_D, Table 4 shows that the Ford et al. (1983) model is the most successful in reproducing experimental K_D·s.

5.3. 0.1 MPa (>9 wt.% MgO) — database

The results of our evaluation using this database are presented in Table 4 and Figs. 3–5. As can be seen from Table 4, both the Ford et al. (1983) and the Herzberg and O'Hara (2002) models are equally as good at calculating experimental temperatures and both are superior to the Putirka (2005) model, which systematically calculates higher temperatures at higher MgO contents (max difference observed is 212 °C, Fig. 3). Again in terms of K_D the Ford et al. (1983) geothermometer is the most successful in reproducing experimental K_D·s.

As can be seen in Fig. 4 the experimental K_D·s display a very significant range with respect to MgO wt.% (Fig. 4a) of the liquid composition and temperature (Fig. 4b). Also shown on Fig. 4, are the calculated trends for K_D·s, MgO wt.% and temperatures by the three olivine geothermometers during incremental olivine addition into the MORB glass from Table 1, resulting in the parental liquid calculations at 0.1 MPa presented in Table 3. For comparison the range in K_D·s calculated using the Toplis (2005) model in combination with the Ford et al. (1983) geothermometer is also shown (see Table 3). Both the Herzberg and O'Hara (2002) and the Putirka (2005) model show increasing calculated K_D·s with MgO (Fig. 4a) and temperature (Fig. 4b). This increase is similar (but displaced to higher K_D·s) to the empirical trend of Sobolev and Danyushevsky (1994) based on high-pressure experiments. However a similar trend is not evident in the dataset as a whole (Fig. 4b). The Ford et al. (1983) model calculates a slightly decreasing K_D with MgO and temperature, cutting across the regression line through the experimental data in Fig. 4a but closely following the regression line in Fig. 4b. The K_D·s calculated by both the Herzberg and O'Hara (2002) and the Putirka (2005) models are offset to higher K_D values compared to both the Ford et al. (1983) model calculations and the majority of the experimental data, as represented by the regression line through the data. In the case of the Herzberg and O'Hara (2002) model this offset is due to the fact that the experimental data used to calibrate their model was based on high-pressure experiments. The Toplis (2005) model calculates almost constant K_D values displaced to significantly lower K_D·s compared to the three geothermometers (Fig. 4).

Thus although the results in Table 4 confirm the Ford et al. (1983) model as the most successful in reproducing experimental K_D·s there is still a very large range of experimental K_D·s leading to uncertainty in deciding, based on experimental data alone, which K_D is appropriate to be used for calculating parental compositions for MORB and Hawaiian compositions at low pressure. In an attempt to resolve this problem, in Fig. 5a and b we have split the data into two groups based on TiO_2 content to get broadly a 'Hawaiian-like' (>1 wt.% TiO_2, Fig. 4a) and a 'MORB-like' (<1 wt.% TiO_2, Fig. 5b) compositions. A simple linear regression of K_D versus MgO for both groups, suggests that a K_D of ~0.32 and ~0.29 is appropriate for MORB and Hawaiian parental liquids respectively (note that a K_D of 0.32 is significantly higher than predicted by Toplis, 2005, see Table 3). The lower K_D inferred for Hawaiian magmas is consistent with the well-known effect of alkalis on lowering the K_D (Falloon et al. 1997; Toplis, 2005). Figs. 4 and 5 also suggest the need for more experimental work to fully understand and predict the K_D value for magmas with >9 wt.% MgO. In light of this uncertainty it is recommended that the Ford et al. (1983) model should be used for olivine addition calculations at 0.1 MPa.

5.4. 1.5 GPa — database

The results of our evaluation using this database is presented in Table 4 and Fig. 6. As can be seen from Table 4 and Fig. 6, both the Ford et al. (1983) and the Herzberg and O'Hara (2002) models are equally as good at calculating experimental temperatures and both superior to the Putirka (2005) model, which systematically calculates higher temperatures at higher MgO contents (max difference observed is 296 °C). In terms of K_D the Ford et al. (1983) geothermometer is equally as good as the Herzberg and O'Hara (2002) model (which is slightly better at predicting high-pressure K_D·s, Table 4). Based on this result any argument concerning the temperatures of mantle plumes relative to MORB based on the Putirka (2005) geothermometer is likely to be incorrect.

5.5. Summary statement — Ford et al. (1983) geothermometer recommended for olivine addition calculations

Based on our evaluations we find that the Ford et al. (1983) geothermometer gives the best overall performance in reproducing experimental temperatures and K_D·s at 0.1 MPa. The Herzberg and O'Hara (2002) geothermometer is equally as good at reproducing experimental temperatures but not as good as the Ford et al. (1983) model in reproducing experimental K_D·s at 0.1 MPa. In general the Herzberg and O'Hara (2002) model will calculate a higher K_D than the experimental value. The Herzberg and O'Hara (2002) model is slightly superior to the Ford et al. (1983) model at 1.5 GPa. Both the Ford et al. (1983) and the Herzberg and O'Hara (2002) geothermometers are superior to the geothermometer of Putirka (2005). The Putirka (2005) model fails to reproduce experimental temperatures accurately and for high MgO liquids, calculates anomalously high temperatures. Studies making petrogenetic statements based on the Putirka (2005) olivine geothermometer therefore should be treated with caution. We recommend that the Ford et al. (1983) olivine geothermometer be used for modelling of olivine crystallization at 0.1 MPa.

6. Application to MORB

In this section we apply the Ford et al. (1983) olivine geothermometer to determine the crystallization temperature of parental MORB liquids at low pressure. In Fig. 7 we present the FeO and MgO contents of 682 MORB glasses from Indian, Pacific and Atlantic spreading ridges (Danyushevsky, 2001). The glass compositions have all been analysed using a Cameca SX50 electron microprobe formerly housed at the Central Science Laboratory, University of Tasmania, Hobart, at 15 kV and 20 ηA, using international standard USNM 111240/2 (basaltic glass) from Jarosewich et al. (1980). In addition all glasses were analysed for H_2O content using FTIR and the techniques of Danyushevsky et al. (1993).

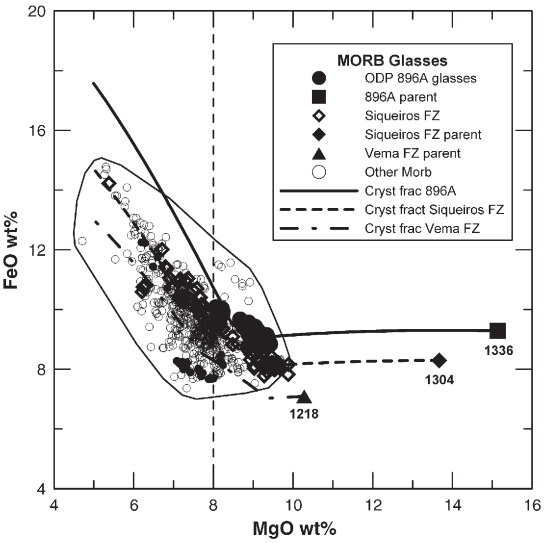

Fig. 7. FeO wt.% versus MgO wt.% for 682 MORB glass compositions (Danyushevsky, 2001). Temperatures of parental compositions are calculated using the olivine geothermometer of Ford et al. (1983) at 0.1 MPa (see text and Table 5 for details). Liquid lines of descent ("Cryst frac") are calculated using PETROLOG software and the method of Danyushevsky (2001).

In Fig. 7, we distinguish two MORB glass suites, for which we have very good mineralogical data on olivine phenocrysts to constrain parental liquid composition calculations: 1) glasses from ODP896A, drilled into ~5 Ma crust formed by the Cocos–Nazca spreading ridge (McNeill and Danyushevsky, 1996); and 2) glasses from the Siqueiros Fracture Zone, East Pacific Rise (Danyushevsky et al. 2003). Also shown on Fig. 7 are parental liquid compositions calculated using the Ford et al. (1983) olivine geothermometer using the most magnesian glass and the most magnesian olivine phenocryst composition observed in each suite (Mg# 91.6 for ODP896A glasses and Mg# 91.5 for Siqueiros FZ glasses). On Fig. 7, shown for comparison, is a parental liquid calculated from the composition of a magnesian olivine glass inclusion from the Vema FZ on the Mid-Atlantic Ridge and the composition of the host olivine (Mg# 90.2) from the study of Sobolev et al.

Table 5
Calculated parental compositions for three representative MORB glasses

	Vema FZ			Siqueiros FZ			ODP896A		
	Glass	Parent (a)	Parent (b)	Glass	Parent (a)	Parent (b)	Glass	Parent (a)	Parent (b)
SiO_2	50.14	49.49	49.3	49.21	48.35	48.07	49.03	47.76	47.49
TiO_2	0.87	0.85	0.83	0.96	0.87	0.84	0.64	0.54	0.52
Al_2O_3	17.94	17.42	17.05	17.02	15.36	14.8	16.07	13.57	13.06
Fe_2O_3	nd	0.48	0.5	nd	0.66	0.7	nd	0.81	0.86
FeO	7.11	6.66	6.72	8.16	7.7	7.74	9.12	8.58	8.59
MnO	0.13	0.13	0.12	0.13	0.12	0.11	0.12	0.1	0.1
MgO	9.6	10.28	11.1	9.89	13.67	14.97	9.43	15.59	16.81
CaO	12.57	12.21	11.95	12.14	10.96	10.56	13.66	11.54	11.1
Na_2O	2.34	2.27	2.22	2.41	2.18	2.1	1.62	1.37	1.32
K_2O	0.06	0.06	0.06	0.02	0.02	0.02	0.02	0.02	0.02
P_2O_5	0.05	0.05	0.05	0.05	0.04	0.04	0.03	0.03	0.02
Cr_2O_3	nd	nd	nd	nd	nd	nd	0.07	0.06	0.06
H_2O	0.1	0.1	0.1	0.07	0.06	0.06	0.05	0.04	0.04
K_D	0.3	0.299	0.32	0.3	0.294	0.32	0.309	0.297	0.32
Oliv Mg#	89.5	90.2	90.2	88.5	91.5	91.5	86.45	91.6	91.6
% Oliv added		1.94	4.04		9.6	12.92		15.58	18.74
T (°C)	1197	1218	1240	1213	1304	1331	1190	1336	1360

Data sources: Vema glass from Sobolev et al. (1989) (Table 1, analysis no. 11); Siqueiros FZ glass, Danyushevsky unpubl data (sample D20–3); ODP896A glass from McNeill and Danyushevsky (1996) (sample no. 896A, 27–1, pc. 15).

(1989). The Vema FZ parent is representative of a relatively low FeO liquid compared with the other parental liquid compositions calculated using the Ford et al. (1983) geothermometer (Table 5). Also presented in Table 5 for comparison are parental compositions calculated using a K_D of 0.32. Note that the parental liquid compositions are more MgO rich and hence hotter when a K_D of 0.32 is used. Fig. 7 also shows a calculated liquid line of descent for each of the calculated parental compositions. Each fractionation path takes into account the effect of H_2O using the method of Danyushevsky (2001). In the case of all three parental suites there is a significant interval of olivine-only crystallization before plagioclase joins the crystallizing assemblage of a ~9 wt.% MgO, and clinopyroxene at ~7.5 wt.% MgO. This interval of olivine-only crystallization is preserved in those relatively rare suites which have high MgO glasses, such as Siqueiros FZ and ODP896A and in the compositions of the most magnesian olivine phenocrysts.

As can be seen from Fig. 7 the MORB glasses display a significant range of FeO contents at a fixed MgO content of 8 wt.%. This range of FeO is clearly correlated with the temperature of parental magmas, with the high FeO glasses derived from more magnesian and hence hotter parental magmas. This range in FeO contents in MORB glasses is a primary feature and cannot be explained by effect of H_2O on low-pressure fractionation path, a possibility suggested by Asimov et al. (2004). The effect of H_2O on crystallization of MORB has been fully discussed by Danyushevsky (2001). The main effect of H_2O on crystallization on MORB is to decrease melt liquidus temperature and to suppress plagioclase crystallization relative to olivine and clinopyroxene. Danyushevsky (2001) demonstrated that even small amounts of H_2O will have significant effect on concentrations of Al_2O_3, FeO and TiO_2. Thus if the effect of H_2O is not taken into account then significant errors will be introduced into FeO_8 calculations, which are frequently used to infer magma generation conditions in the mantle (e.g. Langmuir et al., 1992).

In the case of the high FeO ODP896A glass suite, the parental magma has an olivine crystallization temperature of 1336 °C at 0.1 MPa (1360 °C for a K_D of 0.32, Table 8). In terms of a mid-crustal magma chamber at 0.2 GPa this corresponds to a temperature of ~1345 °C.

It is important to recognize that it is not appropriate for the temperature of parental MORB liquids to be reduced to an average single temperature, such as 1280 °C, commonly quoted for MORB after the study of McKenzie and Bickle (1988) (although this 1280 °C was an average mantle potential temperature). The temperature of the ODP896A parent liquid is significantly hotter than 1280 °C, and also above

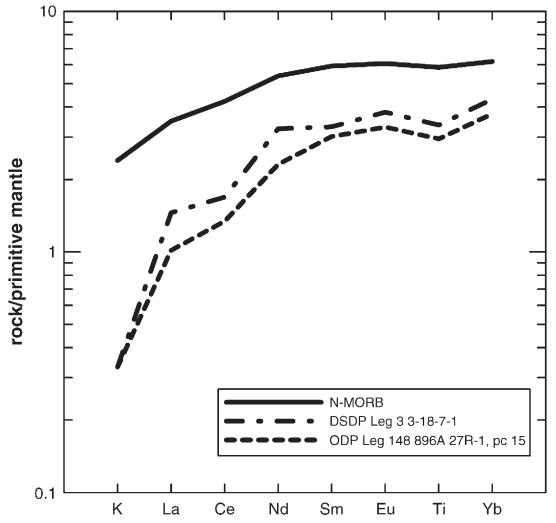

Fig. 8. Normalised abundance patterns for high FeO glass ODP896A 27r-1 pc 15 (Danyushevsky unpubl data) compared to average N-MORB values of Sun and McDonough (1989) and primitive MORB glass from DSDP Leg 3 site 3–18 (Frey et al., 1974). Primitive mantle normalising values from Sun and McDonough (1989).

the range of temperatures inferred for primary MORB magmas (Presnall et al., 2002) from recent experimental studies (average mantle potential temperature required ~1260 °C). Green and Falloon (2005), based on a systematic investigation of MORB glasses with >9.5 wt.% MgO compared with experimental peridotite melt compositions, infer mantle potential temperatures of ~1430 °C for parental compositions such as ODP896A. Although the causes for the range in FeO and MgO contents in MORB glasses can be debated (cf. Klein and Langmuir, 1987), what is important is to recognise is that high FeO glasses, such as ODP896A, which is a typical primitive N-MORB composition (see Fig. 8) are present along all spreading ridges as statistical analysis of Dmitriev et al. (1985) demonstrates. When comparisons are made between crystallization temperatures of parental liquids for Hawaiian and MORB magmas at low pressure, it is the temperatures inferred for the hottest of parental magmas from each suite which should be used to test the 'thermal plume hypothesis'. When such a comparison is done, then the differences between the crystallization temperatures of parental liquids are essentially zero (ΔT ~6 °C, Table 2). Based on this result it is unlikely that significant differences in mantle potential temperatures exist between the mantle sources of MORB and Hawaiian magmatism.

7. Conclusions

A detailed evaluation of the Ford et al. (1983), Herzberg and O'Hara (2002) and the Putirka (2005) olivine geothermometers with experimental data at 0.1 MPa and 1.5 GPa reveals that the Ford et al. (1983) geothermometer is the most successful in reproducing experimental temperatures and olivine-melt K_D's. We therefore recommend that the Ford et al. (1983) olivine geothermometer be used in parental liquid calculations that involve incremental addition of olivine to obtain equilibrium with a target olivine phenocryst composition at low pressure.

The thermometer of Putirka (2005) was found to systematically calculate anomalously high temperatures for high MgO experimental compositions at both 0.1 MPa and 1.5 GPa. This feature of the Putirka (2005) thermometer leads to the different conclusions reached concerning the temperature differences for Hawaiian and MORB mantle sources by the studies of Putirka (2005) and those of Green et al. (2001) and Green and Falloon (2005).

The range in experimental K_D at 0.1 MPa for liquid compositions >9 wt.% MgO is significant, however the data does suggest that Hawaiian magmas due to their higher TiO_2 and alkali contents compared with MORB should have lower K_D (~0.29) values compared with MORB magmas (~0.32). This difference should perhaps be applied when performing incremental olivine addition calculations at 0.1 MPa.

The application of the Ford et al. (1983) geothermometer to calculate the temperatures of crystallization for parental MORB liquids in mid-crustal magma chambers reveals that there exists a ~115 °C temperature range, illustrated by the Vema and ODP896A examples. The hottest MORB parental liquids have crystallization temperatures ~1345 °C (MgO contents ~16 wt.%) for a mid-crustal pressure of 0.2 GPa.

The differences between the olivine crystallization temperatures of the hottest MORB parental liquids and those of Hawaii are essentially zero (ΔT ~6 °C). Thus it is very unlikely that there are significant differences in mantle potential temperatures between their respective mantle sources.

Acknowledgements

We thank Keith Putirka for helpful discussions on some aspects of this work. We also thank Keith Putirka, Peter Ulmer and Marc Norman for constructive reviews.

Appendix A

0.1 MPa experimental data on co-existing melt and olivine pairs from crystallization experiments conducted by Ford et al. (1983) at the University of Edinburgh where the MgO content of the co-existing liquid is >9 wt.% MgO. Details of experimental and analytical techniques are given in Ford et al. (1983). Numbers in parentheses refers to the number of analyses to obtain an average composition for the phase.

No.	Run	T (°C)	Time (mins)	fO_2	Ph.	SiO_2	TiO_2	Al_2O_3	FeOt	MnO	MgO	CaO	Na_2O	K_2O	P_2O_5	Cr_2O_3	NiO
1	MV723 R451	1277	6.5	−6.6	gl	48.67	1.52	14.66	10.93	0.20	9.91	10.23	2.92	0.95			
					ol	40.05			12.37	0.18	46.11	0.42					0.88
2	MV164 R452	1265	16	−6.8	gl	49.19	2.04	14.10	11.49	0.20	9.79	9.04	3.04	1.12			
					ol	40.28			13.48	0.23	45.13	0.31					0.57
3	MV403 R425	1263	7.5	−6.8	gl	49.77	2.01	14.90	11.27	0.11	9.66	8.18	3.03	1.06			
					ol	40.12			14.08		45.40	0.22					0.17
4	MV723 R413	1258	5.5	−6.8	gl	48.88	1.63	14.95	10.37	0.15	9.40	10.23	3.44	0.89			0.06
					ol	39.79	0.02	0.09	12.96	0.16	46.09	0.28					0.60
5	MV109 R523	1265	17	−6.9	gl	46.37	2.77	14.28	11.07	0.19	9.98	10.97	3.11	0.82	0.35	0.09	
					ol	40.14			12.61	0.14	46.29	0.52					0.30
6	MV716 R523	1265	17	−6.9	gl	44.55	3.69	14.09	13.96	0.17	9.94	9.58	2.93	0.67	0.37	0.04	
					ol	39.95	0.15		14.40	0.16	44.51	0.33					0.49
7	ES2058 R523	1265	17	−6.9	gl	47.14	1.98	14.63	11.72	0.18	9.52	10.35	2.73	1.36	0.33	0.05	
					ol	40.36			13.52	0.00	44.90	0.50					0.72
8	MV521 R440	1256	6.5	−7	gl	46.20	2.99	14.32	11.66	0.07	9.83	11.38	2.44	0.99		0.11	
					ol	40.20			12.93	0.23	45.82	0.42					0.40
9	MV403 R555	1261	20	−7	gl	49.79	2.05	14.85	10.98	0.17	9.60	8.28	2.99	0.91	0.32	0.04	0.01
					ol	40.24			13.30	0.22	45.69	0.29					0.26
10	MV403F R555	1261	20	−7	gl	49.73	2.09	14.73	11.09	0.17	9.53	8.36	3.05	1.03	0.17	0.03	0.01
					ol	40.01			13.69	0.19	45.54	0.28					0.29
11	MV106 R441	1245	6	−7	gl	47.70	2.82	15.27	10.88	0.05	9.66	11.09	2.00	0.45		0.07	
					ol	40.05		0.16	13.05	0.12	45.69	0.43					0.50
12	MV166 R426	1250	5	−7	gl	45.57	3.43	13.53	12.01	0.15	9.37	11.87	2.66	1.06	0.34		
					ol	39.92	0.15		14.69	0.20	44.04	0.50					0.51
13	MV166 R427	1243	5	−7	gl	46.29	3.37	13.36	12.04	0.23	9.23	11.58	2.50	1.13		0.26	
					ol	40.46			13.25	0.15	44.84	0.56					0.74
14	MV109 R524	1252	20	−7.1	gl	46.88	2.83	14.33	11.21	0.13	9.51	10.93	2.90	0.81	0.47		
					ol	40.10			12.78	0.17	45.91	0.55					0.50
15	MV716 R524	1252	20	−7.1	gl	45.16	3.90	14.09	13.87	0.19	9.26	9.62	2.93	0.66	0.32		
					ol	39.34			15.48	0.19	44.09	0.31					0.60
16	JCGL0481	1235	17	−7.23	gl	40.80	5.61	9.30	12.93	0.19	9.87	17.91	0.64	1.95	0.67	0.13	
					ol(3)	40.15	0.20		12.68	0.25	45.48	1.05					0.19
17	MV93 R582	1233	4	−7.3	gl	44.08	3.03	13.44	10.10	0.18	9.58	14.95	3.44	0.39	0.70	0.06	0.05
		1233	4	−7.3	ol	40.43		0.14	10.97	0.23	46.99	0.77					0.46
18	JCGL0659	1235	20	−7.38	gl	40.92	5.28	9.35	15.22	0.20	9.72	17.81	0.24	1.21		0.05	
					ol(2)	39.11	0.17		15.31	0.23	43.90	0.94					0.33
19	JCGL0458	1245	20	−7.38	gl	39.08	7.97	8.56	18.44	0.18	9.53	14.35	0.51	1.31		0.08	
					ol	38.90	0.18		16.54	0.26	43.20	0.61					0.31
21	JCGL0682	1204	23	−7.56	gl	42.74	9.15	9.69	9.92	0.20	9.34	15.55	1.30	1.77	0.32	0.03	
					ol(5)	40.74	0.35		10.09	0.27	47.61	0.80					0.14
22	JCGL0627	1210	20	−7.66	gl	41.98	5.64	9.72	13.02	0.23	9.54	18.27	0.13	0.98	0.43	0.07	
					ol(2)	39.75	0.14		13.82	0.18	44.03	0.95					1.12
23	MV166 R560	1270	5	−11.1	gl	46.95	3.24	13.61	11.01	0.23	10.14	11.71	1.90	0.95	0.11	0.15	
					ol	40.02	0.13		14.42	0.12	44.47	0.48					0.36
24	MV106 R561	1255	15.5	−11.2	gl	48.28	2.74	15.54	9.37	0.12	10.04	11.32	1.79	0.59	0.15	0.04	
		1255	15.5	−11.2	ol	40.53			12.66	0.16	46.26	0.39					
25	MV166 R561	1255	15.5	−11.2	gl	47.81	3.41	13.98	10.20	0.20	9.94	11.91	1.68	0.83		0.04	
					ol	40.00	0.14		13.88	0.28	45.09	0.61					
26	MV106 R564	1240	4.5	−11.5	gl	48.17	2.78	15.65	9.77	0.00	9.38	11.33	1.84	0.59	0.42	0.07	
					ol	39.65	0.16		14.08	0.22	45.30	0.44					0.15
27	JCGL0437	1338	20	−6.66	gl (9)	41.94	4.78	8.22	14.41	0.20	14.15	15.84		0.04	0.16	0.21	0.06
					ol (9)	40.32	0.14		11.82	0.19	46.49	0.66					0.38

Appendix A (*continued*)

No.	Run	*T* (°C)	Time (mins)	fO_2	Ph.	SiO_2	TiO_2	Al_2O_3	FeOt	MnO	MgO	CaO	Na_2O	K_2O	P_2O_5	Cr_2O_3	NiO
28	JCGLO237	1338	20	−6.66	gl	39.96	7.27	7.65	17.62	0.18	13.97	12.85		0.31		0.19	
					ol	40.28	0.21		13.25	0.15	45.09	0.64					0.38
29	JCGL0419W-21	1319	3	−6.35	gl	40.74	4.58	8.07	16.19	0.24	13.03	15.51		1.21	0.39	0.05	
					ol	39.54	0.18	0.34	12.47	0.13	46.32	0.85					0.18
30	JCGL0419W-28	1319	3	−6.35	gl	39.48	7.32	7.57	18.14	0.22	12.95	12.85	0.42	0.87	0.17		
					ol(2)	40.00			13.15	0.19	45.77	0.57					0.32
31	JCGL0336	1303	20	−6.67	gl	40.12	7.48	8.25	17.27	0.27	12.64	13.49		0.47			
					ol(4)	40.29	0.21		13.64	0.22	44.73	0.65					0.25
32	ES2058 R527	1321	16.5	−6.2	gl	47.09	1.95	13.53	11.79	0.21	12.33	9.49	2.54	1.01	0.06		
					ol	40.51			11.31	0.18	46.69	0.34					0.96
33	JCGL0553	1302	20	−6.55	gl	40.65	4.78	8.41	16.11	0.23	12.39	16.38	0.12	0.78		0.14	
					ol(5)	39.85	0.13		13.11	0.21	45.51	0.86					0.32
34	JCGL0535	1277	21	−7.14	gl	41.29	5.00	8.64	15.79	0.26	12.18	16.62		0.08		0.14	
					ol(2)	39.88	0.46	0.61	13.03	0.20	44.28	1.28					0.26
35	JCGL0417	1303	3	−6.93	gl	40.51	4.83	8.19	16.01	0.26	12.16	16.15		1.31	0.49	0.09	
					ol(3)	40.00	0.16		12.96	0.18	45.49	0.85					0.36
36	JCGLO453	1302	20	−6.55	gl	40.69	4.79	8.59	15.98	0.16	12.16	16.31		0.79	0.52		
					ol(5)	39.85	0.13		13.11	0.21	45.51	0.86					0.32
37	JCGL0317	1303	3	−6.93	gl	39.24	7.26	7.83	18.52	0.23	11.91	13.00	0.59	1.09	0.33		
					ol(4)	39.90	0.24		14.64	0.18	44.01	0.76					0.28
38	JCGLO454	1294	18	−5.88	gl	41.02	4.91	8.66	15.11	0.23	11.97	16.55	0.28	1.14		0.13	
					ol(5)	40.32	0.14		12.99	0.16	45.19	0.94					0.26
39	JCGL0453	1302	20	−6.55	gl	38.74	7.49	8.18	18.57	0.20	12.04	13.24	0.35	0.98	0.20		
					ol	39.66	0.11		14.49	0.28	44.57	0.65					0.25
40	JCGL0354	1294	18	−5.88	gl	40.75	4.96	8.81	14.98	0.19	11.71	16.48	0.33	1.12	0.44	0.23	
					ol(5)	40.32	0.14		12.99	0.16	45.19	0.94					0.26
41	JCGLO377	1278	16	−6.84	gl	41.41	4.89	14.16	9.85	0.23	11.72	15.55	0.34	1.36	0.42	0.08	
					ol(2)	40.81	0.18		9.41	0.24	48.34	0.78					0.24
42	ES2058 R526-a	1309	19	−6.2	gl	47.15	1.97	13.57	11.96	0.25	11.62	9.92	2.36	1.08	0.12		
					ol	40.66			11.72	0.17	46.29	0.35					0.80
43	JCGL0355	1284	24	−6.53	gl	40.26	5.00	8.63	16.07	0.18	11.63	16.55	0.28	0.97	0.35	0.09	
					ol(7)	39.30	0.26	0.66	13.61	0.27	44.65	0.83					0.41
44	ES2058 R526-b	1309	19	−6.2	gl(2)	47.37	2.01	13.65	11.61	0.22	11.62	9.98	2.27	1.10	0.17		
					ol(2)	40.85			11.28	0.23	46.67	0.34					0.62
45	JCGL0355	1284	24	−6.53	gl	38.72	7.49	8.14	18.93	0.23	11.46	13.38	0.48	1.08		0.09	
					ol(2)	40.03	0.15		15.26	0.19	43.55	0.60					0.21
46	JCGL0255	1284	20	−6.53	gl	39.03	7.65	8.23	17.89	0.20	11.44	13.58	0.59	1.19	0.21		
					ol(2)	39.68	0.17		14.18	0.26	44.63	0.67					0.41
47	JCGL0554	1294	18	−5.88	gl	39.44	7.56	8.07	18.16	0.26	11.48	13.58	0.31	1.12		0.03	
					ol(4)	40.03	0.12		14.65	0.20	44.05	0.62					0.34
48	JCGL0655	1284	24	−6.53	gl	40.76	4.89	8.58	16.39	0.22	11.38	16.65	0.06	1.03		0.04	
					ol	39.96	0.12		13.50	0.25	44.94	0.86					0.38
49	ES2058 R525	1297	22	−6.5	gl	46.90	1.95	13.98	12.17	0.12	11.00	9.84	2.51	1.19	0.17	0.16	
					ol	40.57			12.12	0.25	45.99	0.38					0.69
50	MV403 R497	1288	18	−6.6	gl	49.79	1.91	14.04	11.22	0.15	11.02	8.03	2.74	0.96		0.13	
					ol	40.38			12.27	0.14	46.43	0.24					0.55
51	MV403 R525	1297	22	−6.5	gl	50.15	1.98	13.90	11.36	0.21	11.12	7.84	2.45	0.99			
					ol	40.75			12.01	0.13	46.72	0.39					
52	MV403F R572	1287	4.5	−6.8	gl	49.06	2.00	14.10	11.39	0.17	10.89	7.95	3.12	0.95	0.30	0.03	0.03
					ol	40.27		0.11	12.83	0.20	46.03	0.31					0.25
53	MV403 R572	1287	4.5	−6.8	gl	49.26	2.01	14.16	11.35	0.17	10.83	7.92	3.11	0.87	0.24	0.04	0.02
					ol	40.56			12.61	0.21	45.93	0.29					0.39
54	JCGL0435	1277	21	−7.14	gl	39.11	7.82	8.32	18.13	0.18	10.79	13.79	0.57	0.92	0.24	0.13	
					ol(2)	39.72	0.17		15.47	0.25	43.43	0.66					0.30
55	MV164 R451	1277	6.5	−6.6	gl	48.94	2.11	14.15	11.73	0.16	10.03	8.91	2.92	1.05			
					ol	40.45			13.22	0.17	45.39	0.36					0.42

(continued on next page)

Appendix A (*continued*)

No.	Run	*T* (°C)	Time (mins)	fO_2	Ph.	SiO_2	TiO_2	Al_2O_3	FeOt	MnO	MgO	CaO	Na_2O	K_2O	P_2O_5	Cr_2O_3	NiO
56	ES2058 R521	1287	16	−6.7	gl	47.59	2.03	14.17	11.72	0.17	10.77	10.11	2.21	1.22			
					ol	39.71			12.77	0.20	46.24	0.49					0.59
57	MV723F R547	1277	14	−6.8	gl	48.48	1.57	14.96	10.69	0.19	10.17	9.86	3.15	0.76	0.09	0.06	0.01
					ol	40.53			12.14	0.24	46.56	0.40					0.13
58	JCGL0356	1272	20	−6.89	gl	38.55	7.76	8.15	18.74	0.24	10.68	13.46	0.78	1.18	0.32	0.13	
					ol(2)	39.40	0.22		15.12	0.18	44.06	0.66					0.36
59	JCGL0257	1266	20	−6.85	gl	38.31	7.80	8.41	19.04	0.16	10.47	13.59	0.92	1.13	0.17		
					ol(2)	39.52	0.24		15.41	0.29	43.48	0.75					0.31
60	MV521 R439	1266	7.5	−6.8	gl	46.31	2.90	14.36	11.30	0.16	10.29	11.29	2.33	1.04			
					ol	40.33		0.16	12.23	0.28	46.23	0.45					0.31
61	MV403 R547	1277	14	−6.8	gl	49.43	2.06	14.37	11.18	0.16	10.21	8.13	3.06	0.93	0.43	0.04	0.02
					ol	40.20		0.11	12.92	0.22	45.88	0.30					0.36
62	MV176 R547	1277	14	−6.8	gl	44.98	3.63	13.68	13.68	0.17	10.60	9.41	3.03	0.59	0.21		
					ol	40.04	0.11		13.99	0.19	44.85	0.34					0.48
63	MV403 R451	1277	6.5	−6.6	gl	49.70	1.99	14.23	11.48	0.21	10.09	8.24	2.94	1.06		0.05	
					ol	40.23			13.54	0.13	45.28	0.38					0.44
64	MV164 R451	1277	6.5	−6.6	gl	48.94	2.11	14.15	11.73	0.16	10.03	8.91	2.92	1.05			
					ol	40.45			13.22	0.17	45.39	0.36					0.42
65	MV723F R547	1277	14	−6.8	gl	48.48	1.57	14.96	10.69	0.19	10.17	9.86	3.15	0.76	0.09	0.06	0.01
					ol	40.53			12.14	0.24	46.56	0.40					0.13
66	ES2058 R522	1277	18	−6.8	gl	47.07	2.13	14.23	11.85	0.28	10.04	10.13	2.76	1.22	0.28		
					ol	40.45			13.15	0.24	45.23	0.34					0.59
67	JCGL0224	1446	3	−5.08	gl	40.72	3.78	6.81	15.48	0.21	20.00	12.69		0.20	0.10		
					ol(2)	40.77	0.22		8.65	0.16	49.41	0.61					0.18
68	JCGL0437	1338	20	−6.66	gl(9)	41.94	4.78	8.22	14.41	0.20	14.15	15.84		0.04	0.16	0.21	0.06
					ol(9)	40.32	0.14		11.82	0.19	46.49	0.66					0.38

Appendix B

1.5 GPa experimental data on co-existing melt and olivine pairs from peridotite melting and reaction experiments.

The data presented in Appendix B was obtained in the high-pressure laboratory School of Earth Sciences, Hobart, UTas. Data presented in Appendix B, includes both previously published (Falloon et al., 1999; Falloon and Danyushevsky, 2000) and new data (details will be reported elsewhere). The experimental data at 1.5 GPa was selected based on the following criteria:

1. Excellent mass balance with positive phase proportions for all phases;
2. Experiments that had excellent mass balance were further screened by defining a selection factor based on the differences between calculated (by mass balance) and observed FeO and MgO contents. Experiments with a selection factor of $\sim<|0.5|$ were accepted. This selection factor was necessary as even small errors in FeO and MgO obviously may significantly affect calculated KD's for olivine-melt equilibrium, especially at low melt fractions. This selection factor also helped us to avoid potential problems of quench modification. The empirical selection factor (s.f.) calculated based on wt.% and weight fractions is as follows:

$$\text{s.f.} = \left(\Delta\text{MgO}^{\text{exp-calc}}/\text{MgO}_\text{L} - \Delta\text{FeO}^{\text{exp-calc}}/\text{FeO}_\text{L}\right)\left(\text{f}_\text{L} + \Delta\text{FeO}^{\text{exp-calc}}/\text{FeO}_\text{L}\right)$$

where ΔMgO and ΔFeO are differences between starting experimental and calculated bulk system compositions (using mass balance proportions), MgO_L and FeO_L are measured compositions of the experimental glasses, and f_L is the estimated melt proportion.

Run no.	Temp	Phase	SiO_2	TiO_2	Al_2O_3	FeO	MnO	MgO	CaO	Na_2O	K_2O	Cr_2O_3	Mg# (L)	Mg# (Ol)	K_D
T-4335	1425	gl	49.09	0.61	12.80	7.86	0.19	15.49	12.40	0.99		0.59	78.39		
		ol	40.98			8.22	0.14	49.98	0.34			0.35		91.79	0.325
T-4309	1500	gl	50.34	0.46	10.71	8.10	0.15	19.12	9.51	0.75		0.87	81.32		
		ol	41.11			7.50	0.10	50.49	0.24			0.56		92.54	0.351

Appendix B (*continued*)

Run no.	Temp	Phase	SiO_2	TiO_2	Al_2O_3	FeO	MnO	MgO	CaO	Na_2O	K_2O	Cr_2O_3	Mg# (L)	Mg# (Ol)	K_D
T-4333	1525	gl	51.00	0.36	9.14	8.27		21.35	8.31	0.67		0.89	82.65		
		ol	41.40			6.85	0.13	50.89	0.22	0.00		0.51		93.21	0.347
T-4326	1550	gl	50.28	0.32	8.60	8.31	0.17	22.89	7.80	0.62		1.01	83.58		
		ol	41.19			6.69	0.20	51.19	0.20			0.53		93.40	0.359
T-4332	1375	gl	48.08	0.92	16.23	7.62	0.16	12.89	12.17	1.71		0.22	75.68		
		ol	40.42			9.61	0.11	49.33	0.36			0.17		90.38	0.331
T-4262	1400	gl	48.41	0.65	14.40	7.70	0.15	14.45	12.60	1.25		0.38	77.54		
		ol	41.12			8.42	0.15	49.72	0.32			0.27		91.55	0.319
T-4293	1325	gl	49.16	1.08	18.12	6.91		10.61	10.31	3.80		0.00	73.83		
		ol	40.98			9.73		48.97	0.31			0.01		90.19	0.307
T-4271	1350	gl	48.92	0.98	17.51	7.00		11.50	10.57	3.40		0.11	75.12		
		ol	41.24			9.15		49.20	0.30			0.10		90.78	0.307
T-3569	1480	gl	51.73	0.81	9.50	8.50	0.15	19.41	7.60	1.70	0.31	0.20	80.79		
		ol	41.10			7.40	0.08	51.10	0.22			0.10		92.72	0.330
T-4347	1550	gl	53.81	1.07	5.97	7.89	0.27	22.50	6.48	0.79	0.37	0.86	84.05		
		ol	41.60			5.50	0.15	52.20	0.12			0.43		94.65	0.298
T-4348	1600	gl	54.46	0.72	4.22	7.86	0.29	26.62	4.25	0.44	0.25	0.89	86.25		
		ol	41.72			5.00	0.14	52.62	0.09			0.43		95.17	0.318
T-4350	1510	gl	52.48	1.50	7.27	7.17	0.28	20.40	9.12	0.48	0.40	0.91	84.02		
		ol	41.39			5.75	0.17	51.99	0.21			0.48		94.39	0.313
T-4349	1550	gl	53.37	1.27	6.20	7.50	0.30	22.39	7.20	0.50	0.33	0.95	84.67		
		ol	41.39			5.61	0.13	52.21	0.18			0.48		94.55	0.318
T-4351	1600	gl	53.95	0.88	4.60	7.41	0.28	26.33	5.11	0.35	0.18	0.91	86.82		
		ol	41.45			4.89	0.15	52.93	0.12			0.46		95.31	0.324
T-4302	1400	gl	47.75	0.63	15.48	8.39	0.22	13.45	12.49	1.15	0.21	0.21	74.64		
		ol	40.73			9.33	0.18	49.26	0.33			0.16		90.62	0.305
T-4316	1450	gl	49.02	0.46	12.41	8.12	0.20	16.31	12.01	0.74	0.13	0.60	78.70		
		ol	41.09			8.02	0.14	50.02	0.33			0.40		91.98	0.322
T-4312	1500	gl	50.26	0.31	9.89	8.39	0.20	19.79	9.69	0.56	0.08	0.81	81.29		
		ol	41.06			7.20	0.15	50.85	0.30			0.43		92.87	0.334
T-4314	1500	gl	49.99	0.58	11.60	7.70	0.10	19.20	9.00	1.04		0.80	82.14		
		ol	41.19			6.93	0.06	51.14	0.24			0.43		93.17	0.337
T-4357	1550	gl	50.96	0.39	9.41	7.31	0.10	23.03	7.23	0.74		0.84	85.36		
		ol	41.29			6.01	0.03	51.99	0.18			0.49		94.14	0.363
T-4381	1385	gl	48.50	0.90	15.51	7.20	0.13	13.40	11.90	2.14		0.32	77.39		
		ol	40.82			8.40	0.11	50.13	0.32			0.22		91.63	0.313
T-4376	1370	gl	48.63	1.11	17.20	6.89	0.08	12.01	10.71	3.19		0.17	76.20		
		ol	40.90			8.81	0.07	49.80	0.27			0.16		91.20	0.309
T-4352	1350	gl	48.65	1.22	17.58	6.90	0.10	11.49	10.39	3.56		0.12	75.36		
		ol	40.72			9.10	0.08	49.72	0.27			0.11		90.91	0.306
T-4362	1335	gl	48.96	1.31	17.84	6.64	0.10	11.08	9.92	4.04		0.11	75.41		
		ol	40.89			9.50	0.12	49.09	0.29			0.11		90.43	0.324
T-4343	1325	gl	49.90	1.41	18.70	7.00	0.05	9.10	8.79	5.00		0.06	70.46		
		ol	40.30			11.60	0.05	47.70	0.28			0.07		88.22	0.319
T-3656	1325	gl	49.13	0.69	15.51	8.21	0.11	10.83	13.81	1.40	0.02	0.29	70.76		
		ol	40.50			9.75	0.20	49.00	0.31			0.24		90.18	0.263
T-4311	1500	gl	50.25	0.38	10.41	9.21	0.19	19.02	9.32	0.81	0.01	0.41	79.18		
		ol	41.11			8.02	0.12	50.23	0.25			0.27		92.01	0.330
T-4358	1550	gl	51.14	0.29	8.78	9.11	0.18	22.12	7.22	0.58		0.59	81.75		
		ol	41.24			7.83	0.12	50.35	0.17			0.30		92.21	0.378
C-100	1300	gl	47.12	5.40	16.51	9.30	0.16	7.23	7.80	4.30	2.10	0.07	58.73		
		ol	39.80			14.33	0.15	45.31	0.30			0.11		85.14	0.248
C-89	1350	gl	46.93	3.92	14.71	9.91	0.16	10.21	9.91	3.19	0.83	0.23	65.37		
		ol	40.29			13.03	0.14	45.90	0.40			0.24		86.48	0.295
C-114	1400	gl	48.27	2.83	12.00	9.40	0.15	13.10	11.00	2.39	0.45	0.42	71.89		
		ol	40.33			10.74	0.11	48.13	0.36			0.32		89.10	0.313
T-4319	1450	gl	48.36	2.50	11.53	9.31	0.18	15.12	10.31	1.68	0.43	0.57	74.89		
		ol	40.87			9.41	0.12	48.97	0.30			0.32		90.50	0.313

(continued on next page)

Appendix B (*continued*)

Run no.	Temp	Phase	SiO_2	TiO_2	Al_2O_3	FeO	MnO	MgO	CaO	Na_2O	K_2O	Cr_2O_3	Mg# (L)	Mg# (Ol)	K_D
T-4310	1500	gl	49.88	2.06	9.41	9.11	0.17	18.73	8.21	1.35	0.32	0.75	79.09		
		ol	40.95			8.01	0.10	50.26	0.23			0.45		92.02	0.328
T-4356	1550	gl	50.47	1.56	7.79	8.61	0.17	22.60	6.59	1.08	0.25	0.88	82.89		
		ol	41.05			6.81	0.07	51.46	0.19			0.42		93.32	0.347
T-4359	1550	gl	51.58	0.25	8.20	7.80	0.20	22.90	7.55	0.52	0.06	0.94	84.43		
		ol	41.27			6.31	0.10	51.59	0.17			0.55		93.81	0.358
T-4394	1290	gl	51.51	1.67	19.25	6.35	0.07	7.97	8.09	5.03		0.06	69.70		
		ol	40.58			11.47	0.08	47.46	0.33			0.09		88.29	0.305
T-4386	1300	gl	50.02	1.60	18.91	6.90	0.08	8.89	8.44	5.11		0.05	70.27		
		ol	40.61			10.78	0.10	48.02	0.38			0.10		89.04	0.291
T-3666	1450	gl	50.29	0.58	12.72	7.41	0.08	17.08	9.82	1.39		0.63	80.94		
		ol	41.73			7.54	0.07	50.38	0.27			0.00		92.48	0.345
T-4387	1270	gl	50.07	4.68	18.23	7.01	0.08	6.53	6.11	5.11	2.13	0.06	63.04		
		ol	40.01			13.10	0.15	46.34	0.31			0.09		86.53	0.266
T-4365	1300	gl	47.60	4.90	17.24	8.02	0.09	8.03	7.69	4.82	1.52	0.10	64.72		
		ol	39.95			12.68	0.11	46.84	0.30			0.11		87.03	0.273
T-3637	1400	gl	49.05	2.78	11.96	9.61	0.14	13.08	9.91	2.50	0.54	0.42	71.42		
		ol	41.00			11.43	0.12	47.11	0.34			0.00		88.24	0.333
T-4364	1325	gl	48.49	1.38	18.30	7.70	0.13	9.97	9.66	4.21	0.12	0.05	70.37		
		ol	40.72			10.83	0.15	47.87	0.35			0.07		88.96	0.295
T-4389	1350	gl	48.92	1.31	17.91	7.70	0.14	10.20	9.90	3.85		0.06	70.85		
		ol	40.67			10.59	0.17	48.07	0.40			0.10		89.22	0.294
T-3553	1425	gl	48.93	0.51	13.41	8.51	0.19	14.52	12.31	1.10	0.10	0.42	75.83		
		ol	41.55			9.63	0.17	48.27	0.38					90.16	0.343
T-3542	1450	gl	49.55	0.41	12.21	8.51	0.24	16.62	10.91	0.96	0.08	0.50	78.23		
		ol	41.40			8.74	0.30	49.24	0.32			0.00		91.17	0.348
T-4323	1550	gl	51.26	0.48	6.11	10.81		23.63	6.91	0.31		0.50	80.10		
		ol	40.91			8.02		50.64	0.16			0.26		92.07	0.347
T-4355	1650	gl	49.34	0.25	4.07	10.80		29.90	4.91	0.19		0.53	83.64		
		ol	41.12			6.80		51.72	0.13			0.23		93.36	0.364
T-4400	1500	gl	49.21	0.37	8.72	10.00	0.17	20.61	9.90	0.41		0.60	79.13		
		ol	40.85			8.41	0.16	49.98	0.26			0.35		91.60	0.348
T-4401	1550	gl	52.20	0.24	6.52	10.24	0.21	22.79	6.73	0.37		0.70	80.39		
		ol	41.15			7.19	0.12	51.04	0.16			0.34		92.91	0.313
T-4404	1380	gl	47.37	0.62	15.52	8.81	0.04	13.22	13.12	1.14		0.15	73.36		
		ol	40.67			9.82	0.02	49.02	0.35			0.11		90.12	0.302
T-4403	1400	gl	48.48	0.97	12.03	9.40		14.86	13.10	0.82		0.34	74.38		
		ol	40.62			9.80		49.02	0.34			0.22		90.14	0.318
T-4399	1425	gl	48.12	0.85	10.90	9.50		16.22	13.41	0.57		0.43	75.82		
		ol	40.32			8.82		50.22	0.41			0.24		91.26	0.300
T-4378	1600	gl	52.77	0.80	5.52	6.30	0.22	27.91	4.90	0.44	0.21	0.92	89.18		
		ol	41.71			4.40	0.09	53.22	0.15			0.43		95.80	0.361
T-4363	1550	gl	52.04	1.31	6.01	6.91	0.26	24.42	7.42	0.42	0.34	0.87	86.76		
		ol	41.50			5.15	0.17	52.51	0.23			0.44		95.02	0.343
T-4354	1510	gl	51.01	1.65	7.61	6.78	0.25	21.50	9.25	0.55	0.48	0.91	85.44		
		ol	41.83			5.80	0.16	51.55	0.22			0.44		94.29	0.355
T-4406	1360	gl	48.06	0.55	13.62	9.14	0.17	14.12	13.13	0.95		0.26	73.93		
		ol	40.58			9.87	0.16	48.83	0.35			0.21		90.04	0.314

Appendix C. Addendum: Critical comments on Putirka et al. (this issue)

As requested by the guest editor, we comment on a companion paper Putirka et al. (this issue) which uses a different methodology and model geothermometer to argue for significant excess temperatures between Hawaii and MORB mantle sources. While deriving a significant range of temperatures for parental MORB, they chose to infer ambient mantle T_P from one of the cooler MORB locations at Siqueiros (wrongly stated to be the 'only MOR location where liquids can be traced to an olivine-only fractionation line'), and to compare this with Hawaii. This, and arbitrary choices of depths of melt separation of MORB (0.8 GPa) and Hawaii (3 GPa) add to problems with their methods to bias their

conclusions to extremely high and unrealistic T_P's for Hawaii and model-dependent differences in T_P between MOR and hot-spot settings.

C.1. Olivine-melt equilibrium

The olivine-melt equilibrium model (geothermometer) of Putirka et al. (this issue; Eqs. (2) and (3)) is an improvement on Putirka (2005) model discussed in detail in our paper, however it also has several important problems.

The 2005 version did not recognise the effect of pressure on olivine-melt equilibrium (i.e., according to that model, a composition within an olivine-only field at 0.1 MPa and 2 GPa is implied to have the same olivine liquidus temperature). The 2006 version recognises the effect of pressure, however it does not describe it correctly. It is well known that below ~<3 GPa, the effect of pressure on increasing olivine liquidus temperature is ~5 °C/0.1 GPa (e.g., Ford et al., 1983; Beattie, 1993; Herzberg and O'Hara, 2002). In the Putirka et al. (this issue) geothermometer this effect is ~1.7 °C/0.1 GPa.

The 2005 version described the effect of water on olivine liquidus temperature as a linear decrease of ~15 °C/wt.%. First, the effect of water on liquidus temperature cannot be linear, as clearly follows from the models of H_2O speciation in silicate melts (e.g., Stolper, 1982) and experimental results (see a summary in Falloon and Danyushevsky, 2000). The 2006 version has a larger effect of water, of ~23 °C/wt.%, but it is still linear. The effect is underestimated at low H_2O contents, as experimental data show that 1 wt.% H_2O in a basaltic melt decreases its liquidus temperature by ~70 °C, but is overestimated if applied to high H_2O contents.

The 2005 model significantly overestimated olivine liquidus temperature of high-Mg compositions at both low and high pressures (>100 °C for a picritic composition with ~21 wt.% MgO, see Figs. 3 and 6). Similar calculation using the 2006 model also overestimates such temperatures but to a lesser extent (~65 °C at 1.5 GPa).

Putirka et al. (this issue) also presented a modified Beattie (1993) geothermometer (Eqs. (4) and (5)). The rationale for the modifications is unclear as it is stated that the Beattie (1993) geothermometer is very accurate. The modification resulted in lower calculated temperatures (by 10–15 °C for high-Mg compositions) and a higher effect of pressure (6.1 °C/0.1 GPa vs. 5.5 °C/0.1 GPa) compared to the Beattie model, making the modified model less accurate than the original. The modified Beattie model has a built-in effect of H_2O as in the Putirka 2006 model. The modified Beattie model has a very strong positive effect of pressure on olivine-melt K_D, whereas the Putirka 2006 model has almost none. The modified Beattie model predicts decreasing K_D with increasing melt MgO content, whereas the Putirka 2006 model predicts an increase.

Thus Putirka et al. (this issue) present two very different geothermometers (expressed in Eqs. (2), (3), (4) and (5) respectively), and it is unclear which one is recommended for use.

C.2. Estimation of parental melt compositions

We strongly disagree with the use of whole rock data trends to calculate parental compositions as olivine control lines derived from whole rock data trends do not represent liquid lines of descent (see discussion in Clague et al., 1995, page 330).

Putirka et al. (this issue) use whole rock data trends and olivine compositions to determine K_D's appropriate for MORB and Hawaii (their Fig. 6). This is an inappropriate way of calculating K_D's as 1) rocks do not represent melts (see above) and 2) K_D value is dependent on the ratio of FeO and Fe_2O_3 in the melt. It is not possible to obtain this information from whole rock data in an unequivocal way. Experimental data must be used to constrain appropriate low pressure K_D's (e.g. Stolper et al., 2004; Clague et al., 1995). We have demonstrated that the Ford et al. (1983) model is the best performing geothermometer at low-pressure and have therefore used it to calculate the appropriate K_D's for olivine addition (reverse of olivine fractionation) at low-pressure.

There is abundant evidence from petrological studies of Hawaii tholeiite magmas, that magma chemistry is controlled by low-pressure crystal fractionation (Basaltic Volcanism Study Project, 1981), which is also supported by fluid inclusion studies in olivine phenocrysts from tholeiite series magmas (Anderson and Brown, 1993; Sobolev and Nikogosian, 1994). Therefore Putirka et al. (this issue) are in error by taking a low-pressure olivine composition as a target for the composition of an olivine in the mantle at 3 GPa. As we explained in our paper, compositions of liquidus olivine for a given melt composition are likely to change with pressure, and hence a high pressure olivine is likely to be less Fo rich. For example, a parental liquid for Mauna Loa in equilibrium with Fo 91.3 at 0.2 GPa will be in equilibrium with Fo 90.3 at 2 GPa. If we incorrectly force the parental melt to be in equilibrium with Fo 91.3 at 3 GPa we will add an extra ~50 °C to the calculation.

Putirka et al, (this issue) arbitrarily choose a pressure of 0.8 GPa and 3 GPa as depths of melting for MORB and Hawaii. Depths of melting can only be determined by the

compositions of parental liquids compared to experimental melting studies. This is why it is important to calculate the composition of a parental liquid at low-pressure first, i.e. at conditions where the observed olivine crystallised. This is the approach of Green et al. (2001) and Green and Falloon (2005) who found no significant differences in melting pressure between high-FeO MORB and Hawaii (both ~2 GPa). The "garnet" signature in Hawaii magmas is a source composition feature (Hirschmann and Stolper, 1996; Yaxley and Green, 1998) and is not indicative of the depths of melting.

We note that Putirka et al. (this issue) incorrectly plot (their Fig. 5) and refer to the glass 57-13g as a calculated parental composition and criticise us for its low MgO and high FeO contents. They also incorrectly plot glass 896A from Table 1 and criticise us for its high FeO contents, when in fact its FeO^T content of 9.12 wt.% is identical to the mean MORB FeO^T as plotted by Putirka et al. (this issue) in their Fig. 5. Putirka et al. (this issue) have misread our paper confusing glass compositions with parental liquids. We also note that our use of QFM+0.5 log units for Hawaii is essentially identical (<1% difference) to WM proposed by Rhodes and Vollinger (2005). Consequently the calculated FeO and Fe_2O_3 in our parental liquids and those of Green et al. (2001) are entirely appropriate for Hawaii.

C.3. Passive vs active upwelling

Putirka et al. (this issue) assume that relative buoyancy within the mantle must be attributed to thermal contrasts and disregard all evidence for compositional heterogeneity within the mantle sources for MORB and 'hot-spot' magmas. Density differences within observed lherzolite/harzburgite mantle samples are equivalent to differences of >200 °C if they were to be attributed to potential temperature differences in homogeneous peridotite (Green et al., 2001; Niu et al., 2003). They also appear not to appreciate the dependence of estimates of latent heat of melting on model source and melt fraction assumptions — and estimates of heat of fusion strongly impact on estimates of mantle potential temperature (McKenzie and Bickle, 1988; Langmuir et al., 1992). Thus, inferring melt fraction of >20% at 3 GPa (although inconsistent with residual garnet in pyrolite or PMM source composition) for Hawaii and ~10% at <1 GPa for Siqueiros, ensures that, by the methods used, a higher T_P's will be calculated for Hawaii. Arguments based on trace element abundances for small melt fractions at Hawaii, and/or refertilised harzburgite source, and arguments for depths of partial melting based on experimental studies are ignored.

C.4. Summary statement

The excess temperatures calculated by Putirka et al. (this issue) are an artificial consequence of their methodology and choice of geothermometers. The excess temperatures result from the following:

1) failure to recognise the compositional range within parental MORB and comparison of Hawaiian magmas with low FeO MORB; 2) using whole rock data trends to constrain X_{Mg} of parental liquids; 3) using whole rock data and olivine compositions to determine K_D's; 4) using low-pressure olivine compositions as targets for mantle residue compositions; 5) inappropriate pressures of melting; 6) using a geothermometer which calculates higher temperatures for MgO rich compositions compared to other well calibrated models (Ford et al., 1983; Herzberg and O'Hara, 2002); 7) a very small effect due to H_2O.

In our paper we demonstrate that there is a significant range in temperatures of olivine crystallization for parental liquids to MORB glasses at low-pressures and that there is no significant excess temperature between the hottest MORB and olivine crystallization temperatures of the hottest of Hawaiian liquids (Kilauea Volcano) at low-pressures. Significant differences in mantle T_P's are therefore highly unlikely.

References

Akella, J., Williams, R.J., Mullins, O., 1976. Solubility of Cr, Ti and Al in coexisting olivine, spinel and liquid at 1 atm. Proceedings of the Lunar Science Conference 7, 1179–1194.

Albarede, F., 1992. How deep do common basaltic magmas form and differentiate? Journal of Geophysical Research 97, 10,997–11,009.

Anderson Jr., A.T., Brown, G.G., 1993. CO_2 and formation pressures of some Kilauean melt inclusions. American Mineralogist 78, 794–803.

Ariskin, A.A., Barmina, G.S., 2004. COMAGMAT: development of a magma crystallization model and its petrologic applications. Geochemistry International 42 (Suppl. 1), S1–S157.

Ariskin, A.A., Barmina, G.S., Frenkel, M.Ya., 1987. Simulating low-pressure tholeiite-magma crystallization at a fixed oxygen fugacity. Geochemistry International 24, 92–100.

Ariskin, A.A., Frenkel, M.Ya., Barmina, G.S., Nielsen, R.L., 1993. COMAGMAT: a FORTRAN program to model magma differentiation processes. Computers and Geosciences 19, 1155–1170.

Arndt, N.T., 1977. Partitioning of nickel between olivine and ultrabasic and basic komatiite liquids. Year Book — Carnegie Institution of Washington 76, 553–557.

Asimov, P.D., Dixon, J.E., Langmuir, C.H., 2004. A hydrous melting and fractionation model for mid-ocean ridge basalts: application to the mid-Atlantic ridge near the Azores. Geochemistry, Geophysics, Geosystems 5. doi:10.1029/2003GC000568.

Basaltic Volcanism Study Project, 1981. Basaltic Volcanism on the Terrestrial Planets. Pergamon Press, Inc., New York, 1286 pp.

Beattie, P., 1993. Olivine-melt and orthopyroxene-melt equilibria. Contributions to Mineralogy and Petrology 115, 103–111.

Bender, J.F., Hodges, F.N., Bence, A.E., 1978. Petrogenesis of basalts from the project FAMOUS area: experimental study from 0 to 15 kbars. Earth and Planetary Science Letters 42, 277–302.

Borisov, A.A., Shapkin, A.I., 1990. A new empirical equation rating Fe3+/Fe2+ in magmas to their composition, oxygen fugacity, and temperature. Geochemistry International 27, 111–116.

Boivin, P., 1980. Données expérimentales préliminaires sur la stabilité de la rhönite à 1 atmosphere. Application aux gisements naturels. Bulletin de Minéralogie 103, 491–502.

Clague, D.A., Moore, J.G., Dixon, J.E., Friesin, W.B., 1995. Petrology of submarine lavas from Kilauea's Puna Ridge, Hawaii. Journal of Petrology 36, 299–349.

Danyushevsky, L.V., 2001. The effect of small amounts of H_2O on crystallization of mid-ocean ridge and backarc basin magmas. Journal of Volcanology and Geothermal Research 110, 265–280.

Danyushevsky, L.V., Sobolev, A.V., 1996. Ferric–ferrous ratio and oxygen fugacity calculations for primitive mantle-derived melts: calibration of an empirical technique. Mineralogy and Petrology 57, 229–241.

Danyushevsky, L.V., Falloon, T.J., Sobolev, A.V., Crawford, A.J., Carroll, M., Price, R.C., 1993. The H_2O content of basalt glasses from southwest Pacific back-arc basins. Earth and Planetary Science Letters 117, 347–362.

Danyushevsky, L.V., Sobolev, A.V., Dmitriev, L.V., 1996. Estimation of the pressure of crystallization and H_2O content of MORB and BABB glasses: calibration of an empirical technique. Mineralogy and Petrology 57, 185–204.

Danyushevsky, L.V., Della-Pasqua, F.N., Sokolov, S., 2000. Re-equilibration of melt inclusions trapped by magnesian olivine phenocrysts from subduction-related magmas: petrological implications. Contributions to Mineralogy and Petrology 138, 68–83.

Danyushevsky, L.V., Sokolov, S., Falloon, T.J., 2002. Melt inclusions in olivine phenocrysts: using diffusive re-equilibration to determine the cooling history of a crystal, with implications for the origin of olivine-phyric volcanic rocks. Journal of Petrology 43, 1651–1671.

Danyushevsky, L.V., Perfit, M.R., Eggins, S.M., Falloon, T.J., 2003. Crustal origin for coupled 'ultra-depleted' and 'plagioclase' signatures in MORB olivine-hosted melt inclusions: evidence from the Siqueiros Transform Fault, East Pacific Rise. Contributions to Mineralogy and Petrology 144, 619–637.

Davis, B.T.C., England, J.L., 1964. The melting of forsterite up to 50 kilobars. Journal of Geophysical Research 69, 1113–1116.

Dmitriev, L.V., Sobolev, A.V., Sushevskaya, N.M., Zpunny, S.A., 1985. Abyssal glasses, petrologic mapping of the oceanic floor and "geochemical Leg" 82. In: Bougault, H., Cande, S.C., et al. (Eds.), Initial Reports of the Deep Sea Drilling Project, vol. LXXXII. U.S. Government Printing Office, Washington, pp. 509–518.

Eggins, S.M., 1993. Origin and differentiation of picrite arc magmas, Ambae (Aoba), Vanuatu. Contributions to Mineralogy and Petrology 114, 79–100.

Falloon, T.J., Danyushevsky, L.V., 2000. Melting of refractory mantle at 1.5, 2 and 2.5 GPa under anhydrous and H_2O-undersaturated conditions: implications for high-Ca boninites and the influence of subduction components on mantle melting. Journal of Petrology 41, 257–283.

Falloon, T.J., Green, D.H., O'Neill, H.St.C., Hibberson, W.O., 1997. Experimental tests of low degree peridotite partial melt compositions: implications for the nature of anhydrous near-solidus peridotite melts at 1 GPa. Earth and Planetary Science Letters 152, 149–162.

Falloon, T.J., Green, D.H., Danyushevsky, L.V., Faul, U.H., 1999. Peridotite melting at 1.0 and 1.5 GPa: an experimental evaluation of techniques using diamond aggregates and mineral mixes for determination of near-solidus melts. Journal of Petrology 40, 1343–1375.

Ford, C.E., Russell, D.G., Craven, J.A., Fisk, M.R., 1983. Olivine-liquid equilibria: temperature, pressure and composition dependence of the crystal/liquid cation partition coefficients for Mg, Fe2+, Ca and Mn. Journal of Petrology 24, 256–265.

Frey, F.A., Bryan, W.B., Thompson, G., 1974. Atlantic ocean floor: geochemistry and petrology of basalts from Legs 2 and 3 of the Deep-Sea Drilling Project. Journal of Geophysical Research 79, 5507–5527.

Frost, D.J., Wood, B.J., 1995. Experimental measurements of the graphite C–O equilibrium and CO_2 fugacities at high temperature and pressure. Contributions to Mineralogy and Petrology 121, 303–308.

Gaetani, G.A., Watson, E.B., 2002. Modelling the major-element evolution of olivine-hosted melt inclusions. Chemical Geology 183, 25–41.

Green, D.H., Falloon, T.J., 2005. Primary magmas at mid-ocean ridges, "hot spots" and other intraplate settings: constraints on mantle potential temperature. In: Foulger, G.R., Natland, J.H., Presnall, D.C., Anderson, D.L. (Eds.), Plates, Plumes and Paradigms, Geological Society of America Special Paper, vol. 388, pp. 217–247.

Green, D.H., Ringwood, A.E., 1967. The genesis of basaltic magmas. Contributions to Mineralogy and Petrology 15, 103–190.

Green, D.H., Falloon, T.J., Eggins, S.M., Yaxley, G.M., 2001. Primary magmas and mantle temperatures. European Journal of Mineralogy 13, 437–451.

Grove, T.L., 1981. Use of FePt alloys to eliminate the iron loss problem in 1 atmosphere gas mixing experiments: theoretical and practical considerations. Contributions to Mineralogy and Petrology 78, 298–304.

Grove, T.L., Bryan, W.B., 1983. Fractionation of pyroxene-phyric MOR at low pressure: an experimental study. Contributions Mineralogy and Petrology 84, 293–309.

Grove, T.L., Gerlach, D.C., Sando, T.W., 1982. Origin of calc-alkaline series lavas at Medicine Lake volcano by fractionation, assimilation and mixing. Contributions Mineralogy and Petrology 80, 160–182.

Gudfinnsson, G.H., Presnall, D.C., 2001. A pressure-independent geothermometer for primitive mantle melts. Journal of Geophysical Research 106, 16205–16211.

Gudfinnsson, G.H., Presnall, D.C., 2005. Continuous gradations among primary carbonatites, kimberlitic, melilitic, basaltic, picritic, and komatiitic melts in equilibrium with garnet lherzolite at 3–8 Gpa. Journal of Petrology 46, 1645–1659.

Herzberg, C., O'Hara, M.J., 2002. Plume-associated ultramafic magmas of Phanerozoic Age. Journal of Petrology 43, 1857–1883.

Hirschmann, M., Stolper, E.M., 1996. A possible role for garnet pyroxenite in the origin of the 'garnet signature' in MORB. Contributions to Mineralogy and Petrology 124, 185–208.

Huebner, J.S., Lipin, B.R., Wiggins, L.B., 1976. Partitioning of chromium between silicate crystals and melts. Proceedings of the Lunar Science Conference 7, 1195–1220.

Irvine, T.N., 1977. Definition of primitive liquid compositions for basic magmas. Year Book — Carnegie Institution of Washington 76, 454–461.

Jarosewich, E.J., Nelen, J.A., Norberg, J.A., 1980. Reference samples for electron microprobe analyses. Geostandards Newsletter 4, 257–258.

Kägi, R., Müntener, O., Ulmer, P., Ottolini, L., 2005. Piston-cylinder experiments on H_2O undersaturated Fe-bearing systems: an experimental setup approaching fO_2 conditions of natural calc-alkaline magmas. American Mineralogist 90, 708–717.

Klein, E.M., Langmuir, C.H., 1987. Global correlations of ocean ridge basalt chemistry with axial depth and crustal thickness. Journal of Geophysical Research 92, 8089–8115.

Lin, S.-C., van Keken, P.F., 2006. Dynamics of thermochemical plumes: 2. Complexity of plume structures and its implications for mapping mantle plumes. Geochemical, Geophysical, Geosystem 7, Q03003. doi:10.1029/2005GC001072.

Longhi, J., Pan, V., 1988. A reconnaissance study of phase boundaries in low-alkali basaltic liquids. Journal of Petrology 29, 115–147.

Longhi, J., Walker, D., Hays, J.F., 1978. The distribution of Fe and Mg between olivine and lunar basaltic liquids. Geochimica et Cosmochimica Acta 42, 1545–1558.

Langmuir, C.H., Klein, E.M., Plank, T., 1992. Petrological systematics of mid-ocean ridge basalts: constraints on melt generation beneath ocean ridges. In: Morgan, J.P., Blackman, D.K., Sinton, J.M. (Eds.), Mantle Flow and Melt generation at Mid-Ocean ridges, Geophys. Monogr. Ser., vol. 71. AGU, Washington, D.C., pp. 183–280.

McKenzie, D., Bickle, M.J., 1988. The volume and composition of melt generated by extension of the lithosphere. Journal of Petrology 29, 625–679.

McNeill, A.W., Danyushevsky, L.V., 1996. Composition and crystallization temperatures of primary melts from Hole 896A basalts: evidence from melt inclusion studies. In: Alt, J.C., Kinoshita, H., Stoking, L.B., Michael, P.J. (Eds.), Proceedings of the Ocean Drilling Program, Scientific Results, vol. 148, pp. 21–35.

Montierth, C., Johnston, A.D., Cashman, K.A., 1995. An empirical glass-composition-based geothermometer for Mauna Loa Lavas. In: Rhodes, J.M., Lockwood, J.P. (Eds.), Mauna Loa Revealed: Structure, Composition, History, and Hazards, Geophysical Monograph, vol. 92, pp. 207–217.

Murck, B.W., Campbell, I.H., 1986. The effects of temperature, oxygen fugacity and melt composition on the behaviour of chromium in basic and ultra-basic melts. Geochimica et Cosmochimica Acta 50, 1871–1887.

Nielsen, R.L., 1985. EQUIL: a program for the modelling of low-pressure differentiation processes in natural mafic magma bodies. Computers and Geosciences 11, 531–546.

Nielsen, R.L., 1988. TRACE.FOR: a program for the calculation of combined major and trace-element liquid lines of descent for natural magmatic systems. Computers and Geosciences 14, 15–35.

Nikolaev, G.S., Borisov, A.A., Ariskin, A.A., 1996. Calculation of the ferric-ferrous ratio in magmatic melts: testing and additional calibration of empirical equations for various magmatic series. Geochemistry International 34, 641–649.

Niu, Y., 2005. Generation and evolution of basaltic magmas: some basic concepts and a new view on the origin of Mesozoic–Cenozoic basaltic volcanism in eastern China. Geological Journal of China Universities 11, 9–46.

Niu, Y., O'Hara, M.J., Pearce, J.A., 2003. Initiation of subduction zones as a consequence of lateral compositional buoyancy contrast within the lithosphere: a petrological perspective. Journal of Petrology 44, 851–866.

Parman, S.W., Dann, J.C., Grove, T.L., de Wit, M.J., 1997. Emplacement conditions of komatiite magmas from the 3.49 Ga Komati Formation, Barberton Greenstone Belt, South Africa. Earth and Planetary Science Letters 150, 303–323.

Presnall, D.C., Gudfinnsson, G.H., Walker, M.J., 2002. Generation of mid ocean ridge basalts at pressures from 1 to 7 GPa. Geochimica et Cosmochimica Acta 66, 2073–2090.

Putirka, K.D., 2005. Mantle potential temperatures at Hawaii, Iceland, and the mid-ocean ridge system, as inferred from olivine phenocrysts: evidence for thermally driven mantle plumes. Geochemical, Geophysical, Geosystem 6, Q05L08. doi:10.1029/2005GC000915.

Rhodes, J.M., Lofgren, G.E., Smith, B.P., 1979. One atmosphere melting experiments on ilmenite basalt 12008. Proceedings of the Lunar Planetary Science Conference 10, 407–422.

Roeder, P.L., Emslie, R.F., 1970. Olivine-liquid equilibrium. Contributions to Mineralogy and Petrology 19, 275–289.

Sack, R.O., Walker, D., Carmichael, I.S.E., 1987. Experimental petrology of alkalic lavas: constraints on cotectics of multiple saturation in natural basic liquids. Contribution to Mineralogy and Petrology 96, 1–23.

Sobolev, A.V., Danyushevsky, L.V., 1994. Petrology and geochemistry of boninites from the north termination of the Tonga trench: constraints on the generation conditions of primary high-Ca boninite magmas. Journal of Petrology 35, 1183–1211.

Sobolev, A.V., Nikogosian, I.K., 1994. Petrology of long-lived mantle plume magmatism: Hawaii, Pacific, and Reunion Island, Indian Ocean. Petrology 2, 111–144.

Sobolev, A.V., Slutsky, A.B., 1984. Composition and crystallization conditions of the initial melt of the Siberian meimechites in relation to the general problem of ultrabasic magmas. Soviet Geology and Geophysics 25, 93–104.

Sobolev, A.V., Danyushevsky, L.V., Dmitriyev, L.V., Sushchevskaya, N.M., 1989. High-alumina magnesian tholeiite as the primary basalt magma at midocean ridge. Geochemistry International 26, 128–133.

Stolper, E.M., 1982. The speciation of water in silicate melts. Geochimica et Cosmochimica Acta 46, 2609–2620.

Stolper, E.M., Sherman, S., Garcia, M., Baker, M., Seaman, C., 2004. Glass in the submarine section of the HSDP2 drill core: Hilo, Hawaii. Geochemistry, Geophysics, Geosystems 5, Q07G15. doi:10.1029/2003GC000553.

Sun, S.S., McDonough, W.F., 1989. Chemical and isotopic systematics of oceanic basalts: implications for mantle composition and processes. Geological Society Special Publications 42, 313–345.

Sugawara, T., 2000. Empirical relationships between temperature, pressure, and MgO content in olivine and pyroxene saturated liquid. Journal of Geophysical Research 105, 8457–8472.

Takahashi, E., 1978. Partitioning of Ni^{2+}, Co^{2+}, Fe^{2+}, Mn^{2+} and Mg^{2+} between olivine and silicate melts: compositional dependence of partition coefficient. Geochimica et Cosmochimica Acta 42, 1829–1844.

Takahashi, E., Kushiro, I., 1983. Melting of a dry peridotite at high pressures and basalt magma genesis. American Mineralogist 68, 859–879.

Taylor, W.R., Green, D.H., 1987. The petrogenetic role of methanes effect on liquidus phase relations and the solubility mechanism of reduced C–H volatiles. Special Publication Geochemical Society 1, 121–138.

Toplis, M.J., 2005. The thermodynamics of iron and magnesian partitioning between olivine and liquid: criteria for assessing and predicting equilibrium in natural and experimental systems. Contributions to Mineralogy and Petrology 149, 22–39.

Ulmer, P., 1989. The dependence of the Fe^{2+}–Mg cation partitioning between olivine and basaltic liquid on pressure, temperature and composition. Contributions to Mineralogy and Petrology 101, 261–273.

Ulmer, P., Luth, R.W., 1991. The graphite–COH fluid equilibrium in P, T, fO_2 space: an experimental determination to 30 kbar and 1600 °C. Contributions to Mineralogy and Petrology 106, 265–272.

Walker, D., Kirkpatrick, R.J., Longhi, J., Hays, J.F., 1976. Crystallization history of lunar picritic basalt sample 12002: Phase-equilibria and cooling-rate studies. Bulletin of the Geological Society of America 87, 646–656.

Walker, D., Jurewicz, S., Watson, E.B., 1988. Adcumulus dunite growth in a laboratory thermal gradient. Contributions to Mineralogy and Petrology 99, 306–319.

Weaver, J.S., Langmuir, C.H., 1990. Calculation of phase equilibrium in mineral-melt systems. Computers and Geosciences 16, 1–19.

Yaxley, G.M., Green, D.H., 1998. Reactions between eclogite and peridotite: mantle refertilization by subduction of oceanic crust. Schweizerische Mineralogische und Petrographische Mitteilungen 78, 243–255.